PROJECT FINAL REPORT

Including Graphic Material

Grant Agreement number: *229255*

Project acronym: *3D-NANOBIODEVICE*

Project title: *Three-dimensional nanobiostructure-based self-contained devices for biomedical application*

Funding Scheme: *FP7-CP-FP*

Period covered: *01/07/2009 – 31/06/2012*

Name, title and organisation of the coordinator:

Assoc. Prof. Sergey Shleev

Faculty of Health and Society, Malmoe University, Sweden

Tel: +46406657414; Fax: +46406658100; E-mail: sergey.shleev@mah.se

Name, title and organisation of the scientific representative of the project's coordinator:

Prof. Tautgirdas Ruzgas

Faculty of Health and Society, Malmoe University, Sweden

Tel: +46406657431; Fax: +46406658100; E-mail: tautgirdas.ruzgas@mah.se

Project website address: *www.mah.se/3Dnanobiodevice*

List of Participants

Role	Participant name	Participant short name	Country	Contact person	E-mail address
CO	Malmoe Hoegskola (Malmoe University)	Mah	Sweden	Sergey Shleev	sergey.shleev@mah.se
CR	Novosense AB	NS	Sweden	Fredrik Sebelius	fredrik.sebelius@novosense.se
CR	Aarhus Universitet	AU	Denmark	Duncan Sutherland	duncan@inano.au.dk
CR	Ruhr-Universität Bochum	RUB	Germany	Wolfgang Schuhmann	wolfgang.schuhmann@rub.de
CR	University of Limerick	UL	Ireland	Edmond Magner	edmond.magner@ul.ie
CR	Universität für Bodenkultur Wien	BOKU	Austria	Roland Ludwig	roland.ludwig@boku.ac.at
CR	Consejo Superior de Investigaciones Científicas	CSIC	Spain	Antonio L. De Lacey	alopez@icp.csic.es
CR	Lunds Universitet	ULUND	Sweden	Lo Gorton	lo.gorton@biochem.lu.se
CR	National University of Ireland, Galway	NUIG	Ireland	Donal Leech	donal.leech@nuigalwau.ie
CR	The University of Southampton	US	UK	Phil Bartlett	P.N.Bartlett@soton.ac.uk
CR	Novozymes A/S	NZ	Denmark	Miguel D. Toscano	MTDO@novozymes.com

Abbreviation List

Work Package – WP
Description of Work – DoW
Grant Agreement – GA
Consortium Agreement – CA
Deliverable – D
Exploitation Strategy Seminar – ESS
Milestone – M
Project Coordinator – PC
Management Supporting Team – MST
General Assembly – GA
Gold nanoparticles – AuNPs
Biofuel cell – BFC
Blue multicopper oxidases – BMCO
Laccase – Lc
Bilirubin oxidase – BOx
Glucose oxidase – GOx
Cellobiose dehydrogenase – CDH
Carbon post microarrays – CPM
Direct electron transfer – DET
Mediated electron transfer – MET
Low density graphite – LDG
Ordered assembles of nanoparticles – OAN
Carbon nanotubes – CNTs
Three-dimensional – 3D
General Assembly – GeAs
Nanoporous Gold Chips – NGC
Chemical vapour deposition – CVD
Carbon microfibers – CMF
Graphite rods – GR
Single walled carbon nanotubes – SWCNTs
Multi walled carbon nanotubes – MWCNTs
Cyclic voltammetry – CV
Glucose dehydrogenase – GDH
Intramolecular electron transfer – IET

1. Executive summary

Self-contained wireless bioelectronic devices have huge scientific and practical importance for basic science and for possible applications in medicine, high-tech industry, military, and biocomputing. The anticipation of major breakthroughs in such a range of areas has resulted in significant research focus in such devices together with a rapid growth in the number of publications and patent applications in bioelectronics. The integration of biomaterials with electronic elements, such as electrodes, chips, field-effect transistors, and piezoelectric crystals, yields hybrid bioelectronic systems that may function as **biofuel cells** (**BFC**), biosensors, bioelectronic circuitry, and combinations thereof (Fig. 1). The ultimate technological goal of our project "3D-nanobiodevice" was to construct a hybrid bioelectronic system, viz. potentially implantable self-contained biodevices working in biomatrices of different compositions, e.g. blood, serum, plasma, saliva, extracellular fluids, and cell cultures.

This goal was successfully accomplished. Specifically, at the very end of the project two proof-of-principle wireless self-powered biodevices were fabricated, calibrated, and tested (Fig. 2A). These devices contain glucose or oxygen sensitive biosensors connected to a transmitter/operating electronic device powered by BFCs. Signals from these devices, corresponding to varying concentrations of bioanalytes, are transferred to a back-end system, e.g. a computer with an electronic transducer (Fig. 2B) for storage, processing, and integration of the biological information collected by the biosensors.

The main scientific goal of the project was to enhance understanding of the fundamental principles regarding the control of **electron transfer** (**ET**) reactions between **nanoparticles** (**NPs**), nanotubes (**NTs**), nanofibres, Os and Ru redox complexes, as well as their assemblies confined in ordered **three-dimensional** (**3D**) microscale networks combined with different bioelements, such as glucose oxidising and oxygen reducing enzymes, in order to solve one of the main obstacles of bioelectronics, i.e. the lack of (or poor) electronic communication between the biocomponents and the electronic elements. A number of novel 3D nanobiodevices were designed and tested, such as glucose and oxygen sensitive microbiosensors, nanostructured biocathodes and bioanodes, and their combinations with electronics (operating unit containing transmitter, potentiostat, electric power storage device and transducer) into autonomous and self-contained, potentially implantable devices powered by 3D biofuel cells. Theoretical modelling of the response of the sensors combined with a detailed experimental characterisation of the properties of the sensors were performed in glucose containing biological matrices of different composition and pH, e.g. blood, plasma, serum, and saliva. The required long-term, operational stability of the 3D nanostructured biodevices was achieved by choosing the appropriate bioelements from already available and from novel wild-type and specifically engineered highly active, stable, and halide resistant redox enzymes, such as **glucose oxidase** (**GOx**) and **cellobiose dehydrogenase** (**CDH**), as well as high redox potential **blue multicopper oxidases** (**BMCO**).

The self-contained biodevices that we developed are still macroscale in size. However, their miniaturisation is possible and such miniaturised biodevices can be used for continuous glucose and oxygen monitoring in different parts of the human body, thus improving the quality of life and increasing patient safety for such chronic conditions as diabetes and methemoglobinemia. Moreover, in the long-term, wireless self-powered biodevices based on nanobiostructures might be used for neuron/nerve stimulation to compensate or alleviate the effect of human disabilities as well as to treat chronic pain, cerebral palsy, and other conditions.

Beside the scientific and technological work, significant disseminative activities were carried out by the Consortium. In addition to classical dissemination roots (publications in journals, conferences, symposiums, and congresses) and novel/electronic means (web), results from "3D-nanobiodevice" were used in lectures, education programs (summer schools, workshops, and colloquiums), and other communication materials (newsletters, flyers, posters) transmitted via mass communication media.

2. Summary description of the project context and the main objectives

FP7 R&D project "3D-nanobiodevice" entitled: "Three-dimensional nanobiostructure-based self-contained devices for biomedical application" has been focused on several scientific, technological, and social objectives simultaneously.

One of the main scientific objectives was to enhance the understanding of the fundamental principles for controlling electron transfer reactions between **gold NPs** (**AuNPs**), **carbon NTs** (**CNTs**), **carbon post materials** (**CPMs**), **conductive nano/-microporous silicone and silicate** (**NMPSi** and **NMPSiT**) chips, their assemblies confined into 3D microscale networks, and different bioelements, such as glucose oxidising (**GOx** and **CDH**) and oxygen reducing (laccase (**Lc**) and **bilirubin oxidase** (**BOx**)) enzymes.

Another important scientific objective of the project was to understand experimental limits and fundamental differences in the performance of 3D nanobiostructures in different biomatrices, specifically human physiological fluids and cell based in vitro platforms versus simple buffer solutions.

The main technological objective of the project was to construct potentially implantable self-contained wireless biodevices for glucose and oxygen monitoring (Fig. 1). Novel biodevices were constructed by combination of glucose and oxygen sensitive biosensors made from 3D nanobiostructured materials, and operated by an electronic unit containing a transmitter, operating system, potentiostat, and an electric energy harvesting device (Fig. 2A).

The last but not the least objective of the Project, strongly oriented towards nanotechnology and biotechnology, which have usually topped most lists of areas where the "next-big-thing" would come from, is an intensive and fair communication with the scientific community and the public at large, in full agreement with the EC strategic roadmap on communicating nanotechnology.

All scientific, technological, and disseminative objectives of the project were successfully accomplished as described in detail below. It is important to emphasise that the scientific and technological objectives of "3D-nanobiodevice" lie somewhere between these two applications (Fig. 3). By integrating fabricated nanobiostructure based biodevices and electronic elements into functional biomedical devices with a wireless transmission feature and testing the proof-of-concept for wireless glucose and oxygen sensing in real biological fluids, "3D-nanobiodevice" project stepped far beyond the state-of-the-art.

Nanowiring of appropriate redox enzymes with AuNPs, CNTs, CMPs, proper surface modifications, and use of Os and Ru redox complexes, were chosen as a major direction to solve main obstacles in the area of bioelectronics, *i.e.* poor electronic communication between the biocomponents and the electronic elements along with insufficient operational stability. To produce 3D bioelectrodes with superior characteristics mathematical modelling of their performance was performed and the results obtained from calculations were compared against experimentally determined parameters. From the modelling and characterisation results, optimisation of the biodevices (glucose and oxygen sensitive biosensors, bioanodes, and biocathodes) was done to increase their efficiency and stability.

Such an ultimate technological goal, as the construction of potentially implantable self-powered wireless biodevices working in biomatrices of different compositions and pHs, could be achieved

only in the very end of "3D-nanobiodevice". The final outcome of the project has been broken down to smaller tasks, which can be divided into seven main groups:

(1) development of electronic parts of the devices, their combination into the functional transmitter/receiver system, and development of the requisite software (Fig. 4),
(2) fabrication of stable 3D-nanostructures (Fig. 5),
(3) production of active bioelements (Fig. 6),
(4) design of Os or Ru containing redox polymers (Fig. 7),
(5) combination of nanostructures and redox enzymes into efficient nanostructured biomodified electrodes, which could serve as glucose and oxygen sensitive biosensors, sugar oxidising bioanodes, and oxygen reducing biocathodes,
(6) fabrication and characterisation of **direct ET** (**DET**) and **mediated ET** (**MET**) based BFCs,
(7) design and testing of self-contained biodevices for glucose and oxygen monitoring.

Indeed, these scientific and technological steps were successfully reached by the Consortium as detailed below:

1.1. Development of a wireless transmission system with voltage multiplayer converting 0.57 V to 2.5 V integrated with capacitive power storage
1.2. Design of a micro-potentiostat integrated with glucose and oxygen biosensors and wireless transmission system
1.3. Creation of a data transmission system with optimised data transfer and antenna for data transfer over distances of more than 3 meters
1.4. Development of optimised hardware and software components as a basis for a self-contained measurement-transmitting device

2. Electroconducting 3D nanoarchitectures were fabricated and characterised morphologically and electrochemically:
2.1. NMPSi and NMPSiT chips of area 6x6 mm^2 and of depth 10-100 μm
2.2. **Ordered assembles of NPs** (**OAN**) with NPs sizes varying from 2 to 200 nm
2.3. **Hierarchical two-generation CNTs based materials** (**HTGCNT**) 10-100 μm deep
2.4. CPM arrays with 6x6 mm^2 areas and 10-100 μm deep structures
2.5. Mesoporous gold electrodes

3.1. Available glucose oxidising and oxygen reducing enzymes were isolated on preparative scale (up to 500 mg), purified to homogeneity, and characterised biochemically and kinetically:
3.1.1. Anodic bioelements: both GOx and CDH, > 100 mg
3.1.1. Cathodic bioelements: BMCO, *viz.* Lcs and BOx, > 100 mg
3.2. Newly screened and designed bioelements were produced, purified, and delivered to the consortium:
3.2.1. Anodic bioelements: both GOx and CDH, > 50 mg
3.2.2. Cathodic bioelements: chloride resistance high redox potential Lcs, > 50 mg

4. Os or Ru containing redox polymers were produced, tested, and delivered to consortium. A large library of redox polymers was also designed (Fig. 7)

5. 3D biodevices functioning as glucose and oxygen sensitive biosensors, sugar oxidising bioanodes, and oxygen reducing biocathodes, were fabricated by biomodification of 3D nanostructures with suitable bioelements (Fig. 8).

6.1. Unoptimised DET and MET based BFCs were fabricated based on available bioelements. The biodevices were characterised in simple buffer solutions and human physiological fluids, e.g., human serum.

6.2. Optimised DET and MET based BFCs were designed based on fabricated electroconducting 3D nanoarchitectures modified with novel engineered bioelements. The performance of biodevices was tested in simple buffer solutions and human physiological fluids, e.g., human blood, plasma, serum, and saliva.

7. Two wireless self-powered biodevices for glucose and oxygen monitoring were designed and tested (Fig. 2).

In addition to technological tasks the fundamental principles of the function of electroconducting biodevices based on 3D nanobiostructures were studied and some experimental limits in their performances were clarified as described below:

1. Efficient motionless 3D nanobiostuctures based biodevices for oxygen reduction perform in mass-transfer limited regime, i.e. with maximal current densities up to 0.5 mA cm^{-2}, whereas most CDH modified bioelectrodes were limited by the activity of redox enzymes immobilised on the electrode surface. Contrary to CDH modified electrodes, some GOx modified 3D nanobiostructures also operate in mass-transfer limited regime, i.e. with maximal current densities up to 5 mA cm^{-2}.

2. Most of the 3D nanobiosturctures based biodevices for glucose oxidation operated at quite high potentials (up to 0.5 V vs. NHE), which is not suitable for biosensing purposes and BFC applications. Several possibilities to decrease the overpotential for sugar oxidation of CDH- and GOx modified 3D electrodes were undertaken, viz. mutagenesis of redox enzymes and appropriate choice of redox mediators using a design library of Os and Ru containing redox polymers (Fig. 7). Contrary to CDH- and GOx modified electrodes, motionless 3D nanobiostuctures based biodevices for oxygen reduction operated at potentials very close to redox equilibrium potentials of the oxygen/water couple at certain conditions (e.g. 0.7 V vs. NHE at physiological pH values).

Another scientific objective of "3D-nanobiodevice" entailed the investigation of fabricated and characterised 3D-nanobiostructures in human blood, plasma, saliva, and cell based in vitro platforms *vs.* simple buffer solutions. Specifically:

1. Needed equipment for investigation of human physiological fluids were installed, volunteers (donors) were identified, and samples were collected (Fig. 9). This was done in accordance with ethical issues and biomedical protocols presented in detailed project description (Annex I).

2. Investigations of designed nanobiostructures in blood, plasma, serum, and saliva were performed (Fig. 10). It was shown that 3D bioelectrocatalytic structures for oxygen electroreduction lose efficiency and stability in complex physiological fluids because of the inhibition/deactivation of redox enzymes (Lc and BOx) by different organic and inorganic substances. In addition, electrochemical oxidation of different interfering compounds, primarily ascorbate occurred on the nanostructured electrodes. Two major strategies towards overcoming the expected limitations of biocathode performance can be proposed, viz. (i) blocking of the bare nanostructured surface to disable direct contact with interfering molecules and (ii) use of another electrode material, which is inert with regard to ascorbate electrooxidation. The latter approach is quite difficult to realise since interfering molecules, e.g., ascorbate, can be efficiently electrooxidised at quite low overpotentials on most conductive electrodes. To block ascorbate molecules from bare surfaces, negatively charged polymers can be used. However, a significant efficiency decrease of the essentially

membrane based biocathode compared to membrane-less biodevices is expected, owing to mass-transfer limitations. Thus, one of the best approaches is to block nanostructured surfaces with a dense monolayer of a biocatalyst using oriented enzyme immobilisation on modified electrode surfaces, as has been already done in the case of Lc-based biocathodes (Partner CSIC).
In contrast, glucose oxidising 3D-nanobiostructures can, in principle, be activated by inorganic compounds, e.g. calcium ions, as was shown by Partner ULUND. However, the concentration of these compounds in human fluids is not sufficient to enable activation, while the low substrate content of biofluids (glucose, lactose, etc.) resulted in quite inefficient performance of CDH-based nanobiostructures. One of the possible solutions to improve efficiency of bioanodes in physiological biomatrices is the use of even more efficient biocatalysts, e.g., engineered CDH with low K_M and high k_{cat} values for glucose. Another approach is to increase the coulombic efficiency of anodic biodevices. The majority of currently developed biodevices extract only two electrons from glucose or lactose molecules, while much more is really possible. For instance, complete oxidation of glucose can give 24 electrons and thus approaching complete oxidation of glucose is important scientific challenge into improving the power output from bioanodes operating in energetically poor (with low amount of biofuels, e.g., glucose) physiological fluids, e.g., human saliva.

Additional testing of biomodified electrodes was performed in cell culture conditions (Fig. 11) to investigate their biocompatibility. For this purpose, oxygen reducing and glucose oxidising biodevice were designed in cell culture plates containing a permeable membrane at the bottom (Fig. 11.1). The system was created by using disposable electrode arrays, 8W2x1E (Applied Biophysics, USA) which were modified prior to investigation biodevices. Each array contained eight wells with two planar gold electrodes each (Fig. 11.1). The construction and the performance of the biodevices were optimised for several days by monitoring of both analytes under cell culture conditions. The catalytically inactive elements of biodevices, e.g. non-biomodified nanostructured surfaces based on CNTs, did not affect attachment and growth of cells on the surfaces (Fig. 11.2). However, the introduction of biocatalysts, e.g., GOx or BOx enzymes rendered the surfaces strongly cytotoxic even when the biodevices were not electrically connected (Fig. 11.2). The effect of GOx can be easily explained by the generation of hydrogen peroxide at GOx modified surfaces since both substrates of the enzyme are present in the solution, glucose and oxygen. In case of BOD the result cannot be explained by BOx catalytic reaction since in the absence of electron donors (without applied potential) the enzyme does not function. Further investigations are needed to understand the cell toxicity of the nanobiostructured surfaces.

It should be emphasised that wireless self-powered 3D nanobiostructure based devices developed in the frame of the project are still macroscale (Fig. 2). Moreover, miniaturisation of electronics is also need. However, the results of the project including proof-of-principle tests show, without a doubt, that miniature self-contained biodevices can be used for continuous glucose and oxygen monitoring in different parts of the human body, thus improving quality of life and increasing patient safety in the case of widely prevalent chronic diseases such as diabetes and methemoglobinemia. Moreover, in the long term, 3D nanobiostructure based elements will be essential for constructing devices to be used for neuron/nerve stimulations and compensation of human disabilities.

Besides scientific and technological work strong communication activities were carried out by the Consortium. In addition to classical dissemination roots (publications in journals, conferences, and workshops) and novel/electronic means (web), results from “3D-nanobiodevice” were used in lectures, education programs, and other communication materials (newsletters, flyers, posters) via mass communication media.

3. Main S & T results/foregrounds

All the work of the Consortium has been done in strict observance with the structure of Annex I of the **Grant Agreement** (**GA**) following the project objectives and **description of work** (**DoW**). The detailed plan of the work was described in five **workpackages** (**WPs**).

WP1. Fabrication and characterisation of microscale 3-D electrodes (AU, RUB, UL, ULUND).

One of the main aims of this WP was to produce conductive, high surface area supports for the immobilisation of enzymes for use in biosensors and BFCs. High surface area supports are essential for the successful immobilisation of enzymes at loadings that can deliver the current and power requirements of the devices needed for self-contained wireless bioelectronic devices. The main objective of this work package was to produce conducting 3D nanostructures with controlled nanodimensions, surface chemistries and surface energies/curvatures for efficient performance of enzymes in 3D nanostructures. Four approaches were planned: (i) the fabrication of carbon post materials (CPM), (ii) the formation of conductive NMPSi and NMPSiT chips, (iii) the synthesis of **hierarchical two-generation carbon nanotube materials** (**HTGCNT**) grafted onto graphite electrodes and (iv) the fabrication of **ordered assembles of nanoparticles** (**OAN**) and **nanoporous gold chips** (**NGC**). Devices using each of these approaches have been prepared and characterised as described in the following sections.

(i) CPM (ULUND)

CMPs were prepared using adaptations of methods previously described (Wang at al 2004; Xu at al., 2007) to prepare electrodes that were suitable for use in a BFC. A schematic diagram of the procedure is shown in Fig. 11. At the start of the project, silicon was used as substrate for the pillars (Fig. 12), however the first layer cracked in the pyrolysis step due to the high stress build up in the resist during baking and subsequent pyrolysis. Due to the low sample yield on silicon caused by cracking, graphite was used instead, producing a higher yield. This is likely due to the fact that graphite has a rougher surface which acts as an anchor for the resist. As graphite is also a better electrical conductor, all subsequent arrays were prepared using graphite. Samples were mounted on printed circuit boards (Fig. 13). The electrodes were plasma treated for 45 sec in O_2 plasma in a Plasma Preen II to create hydrophilic surfaces. Electrochemical characterisation was performed using ferricyanide and ruthenium hexamine and showed that the arrays had a surface roughness factor of 3. Batches of electrodes were examined as enzyme supports. The results of these experiments demonstrated that high loadings of enzymes were not achieved and that the CMP arrays were not suitable supports for use in BFCs.

(ii) NMPSi and NMPSiT chips
NMPSi (Mah)
Double-sided three-dimensional porous silicon chips, 6×6 mm, covered with a 40 nm gold (nano)layer, were fabricated from a porous silicon wafer (Figure 14). Scanning electron microscopy along with electrochemical characterisation showed sample conductivity, mechanical stability, and high surface area of the thus fabricated devices, *viz.* ten times higher electrochemically active surface area compared to the geometric area. The three-dimensional gold coated silicon chips were further modified with thiol layers, followed by immobilisation of a simple copper-containing redox protein, azurin, or a complex multicopper redox enzyme, laccase. The bioelectrochemical studies showed very high surface concentrations of azurin and laccase, *i.e.* close to the theoretical monolayer coverage. However, direct electron transfer reactions between the biomolecules and gold surfaces were observed only for a small percentage of the immobilised redox protein and enzyme,

respectively. Thus, highly efficient oxygen-bioelectroreduction on laccase-modified 3D thiol-gold-porous silicon chips (as compared to planar laccase-modified gold electrodes, 42 μA/cm^2 versus 7 μA/cm^2, respectively) was obtained only in the present of an efficient soluble redox mediator. Thus, NMPSi chips were excluded from further studies due to the relatively low rates of direct electron transfer which rended the material unsuitable for device fabrication.

NMPSiT (UL)

Fluorinated tin oxide (FTO) electrodes (dimensions 2 cm x 1 cm) were modified with a thin layer of mesoporous silicate with the pores orientated orthogonal to the electrode surface. A scanning electron microscopy image of the hexagonal arrangement of the silicate mesopores is presented in Fig. 15. Electrochemical studies, coupled with SEM images demonstrate that the pores of the materials are perpendicular to the surface of the electrode. The thin films were stable at pH of 4 or less. The silicates degraded at pH 7, the experimental condition where most enzyme immobilisation is performed. This instability significantly reduces the use of the films for bioelectrochemical applications and as a consequence, attention focussed on the preparation and characterisation of porous gold electrodes (vide infra).

(iii) HTGCNT (RUB)

Hierarchical carbon nanotubes composite electrodes were fabricated by pretreatment of ordinary graphite rods (of 3 mm diameter; Fig. 16A) using a two-step **chemical vapour deposition** process (**CVD**). Iron clusters were deposited using various electrochemical deposition conditions and techniques (cyclic voltammetry and pulse voltammetry), functioning as local catalysts for the deposition of carbon The first step consisted in growing **carbon microfibers** (**CMF**) of approximately 7 μm in diameter (Fig. 16B) and of 500-3000 μm in length, using a top temperature of 1150 °C and methane as carbon source. CMF were firmly anchored to **graphite rods** (**GR**) and to enable electrical conductivity between the surface of CMF and the GR. A second iron catalyst deposition step was performed on the GR/CMF structure to grow **multi walled carbon nanotubes** (**MWCNTs**) at a temperature of 750°C, using acetylene as the carbon source (Fig. 6C and 6D). The individual characteristics of the synthesized MWCNTs in terms of density, length and diameters were highly dependent of individual conditions experienced by each GR/CMF rod within the same fabrication batch. In spite of these variations, the resultant GR/CMF/MWCNTs composite electrodes demonstrated excellent electrical conductivity throughout the composite structure. From electrochemical modification of GR/CMF/MWCNTs with anthraquinone derivative studies at US, a large increase in the surface area of the electrode of approx. 200 was observed. Over 1000 composite electrodes were fabricated and distributed among partners of the consortium. Extensive bioelectrochemical studies using these composite electrodes as 3D-electrified interfaces were performed at RUB, CSIC, and US. A large number of composite electrodes (> 40) were also used for fabrication and testing of various electrode designs during the experimental session in RUB, carried out during the final project meeting.

(iv) OAN (AU) and NGC (UL)

Nanoporous gold electrodes were prepared by de-alloying a gold silver alloy in 70% (w/v) nitric acid heated to 40°C for 15 minutes. The alloy was prepared by co-sputtering gold and silver onto a gold (300 nm) and titanium (10 nm) coated glass slide. Two different types of mesoporous gold electrodes were prepared, labelled “increasing” and “constant” mesoporous gold with higher amounts of silver deposited and equal amount of silver and gold deposited, respectively. The electrodes were fully characterised using a range of electrochemical, microscopic and spectroscopic methods. Using gold oxide formation to probe the surface areas, surfaces area 28 and 16 fold higher than that of planar gold were determined for increasing and constant mesoporous gold, respectively. Using the redox protein, cytochrome c, the bioelectrochemically addressable electrode surface area was determined to be 11 and 9 times higher for increasing and constant mesoporous gold,

respectively. Batches of electrodes were prepared (40 electrodes per batch) and shipped to RUB, ULUND, CSIC, and NUIG. The electrodes have been used as supports for a range of enzymes, including CDH, GOx, Lc, and BOx.
Different types of ordered arrays of nanoparticles (OANs) were developed by using the polymer polydiallyldimethylammonium chloride (PDDA) and AuNPs causing the nanoparticles to self-assemble into an array. Glancing angle deposition was used to grow the nanoparticles into pillars, thus increasing the surface area considerably. After fabrication the samples were characterised with a variety of methods including scanning electron microscopy (Fig. 17) and **cyclic voltammetry** (**CVs**). Several enzymes including GOx bind to the surface of the samples, while retaining the activity of the enzymes. Bioelectrocatalytic responses were observed when using soluble mediators, but none of the structures showed any direct electron transfer response in the absence of mediators. While these structures may have potential applications in extra vivo sensors, they are not suitable for implantable sensors and were not explored further.

WP2. Engineering of bioelements by rational design and directed evolution (BOKU, CSIC, NZ, INBI).

The contribution of WP2 to the project involved the production of existing glucose oxidizing (anode) and oxygen reducing (cathode) enzymes, as well as new wild-type enzymes obtained by screening, and the development of protein engineered variants with improved properties. The aim of this WP is to provide the consortium with the best bioelements to design efficient and stable BFCs, as well as sensitive and selective biosensors.

As a starting point, a collection of known enzymes was produced in purified form (at ~100 mg scale) and supplied to the consortium partners for initial testing (Fig. 5). These included a variety of **CDH from *Myriococcum thermophilum*** (***Mt*CDH**) and ***Humicola insolens*** (***Hi*CDH**), and also the well-known **GOx from *Aspergillus niger*** (***An*GOx**), which has been used in several commercial glucose biosensors. This set of enzymes has a wide range of properties (pH, glucose activity, thermal stability) and allowed for the construction and testing of bioanodes and glucose sensitive biosensors utilising both MET and DET systems, under different reaction conditions, as well as different immobilization strategies. For testing the construction and initial performance of biocathodes, **Lcs from *Myceliophthora thermophila*** (***Mt*Lc**), ***Streptomyces coelicolor*** (***Sc*Lc**), ***Trametes hirsuta*** (***Th*Lc**), ***Rhus vernicifera*** (***Rv*Lc**), as well as a **BOx from *Myrothecium verrucaria*** (***Mv*BiOx**), were produced, purified, and sampled. These enzymes also cover a range of characteristics, with high-, medium- and low-redox potential enzymes, of different pH optima and susceptibility to chloride ions (a common issue with laccase-based systems). Despite the variety observed in this set of available enzymes, there were a number of limitations of the bioelements that needed to be overcome to obtain an optimal bioelectrode working under physiological conditions (pH 7.4, glucose concentration of ~5 mM and chloride concentration of ~150 mM). These limitations were addressed by screening for new wild-type enzymes, as well as optimising performance of the best available enzymes by protein engineering.

The sourcing of new wild type enzymes commenced using a Prussian blue-based screening assay for novel carbohydrate oxidoreductases with improved glucose turnover at pH 7.4. This process was successfully developed and validated by the subcontractor Prof. M. Rabinovich from the A.N. Bach Institute of Biochemistry, Moscow. In the following screening of several hundred fungal cultures 15 carbohydrate oxidoreductase producing fungal species were identified (Fig. 18) of which 7 were characterized and the results published (Harreither et al., 2011; Sygmund et al., 2011a). Of these enzymes, six were CDHs and one an FAD-dependent **glucose dehydrogenase** (**GDH**). After

investigating the molecular and catalytic properties *Mt*CDH, ***Dichomera saubinetii* CDH** (***Ds*CDH**), and ***Corynascus thermophilus* CDH** (***Ct*CDH**) and **GDH from *Glomerella cingulata*** (***Gc*GDH**) were produced on a large scale (~300 mg) and distributed to the cooperating partners for testing in combination with existing electrodes. These CDHs have a significantly improved glucose turnover at pH 7.4 compared to the previously available basidiomycetous CDHs (Harreither et al., 2012).

Further improvements of DET-anode biocatalysts were pursued by means of genetic engineering using a rational, structure-based approach. *Mt*CDH was successfully used as template to improve the **intramolecular electron transfer** (**IET**) between the flavodehydrogenase domain and the cytochrome domain to achieve an overall faster electron transfer from the substrate to the electrode (Fig. 19). The main steps in this process were the comparative modelling of the enzyme's structure, docking experiments to evaluate the domain interaction, the identification of factors increasing the IET, site-directed mutagenesis, recombinant production in the expression host *Pichia pastoris*, purification by a multi-step chromatographic procedure, steady-state and transient-state kinetic measurements, and finally the evaluation of the obtained enzyme variants. Beneficial mutations were combined and final variants carried up to seven mutations which increased the IET up to 3.5-fold. In another subtask the glucose turnover in *Mt*CDH and *Ct*CDH was increased by mutating the active site and a combination of certain mutations. The catalytic efficiency of both CDHs for glucose turnover was increased by a factor of 5. Additionally, the catalytic efficiency for maltose, which is an interfering substance for glucose biosensors, could be reduced 100-fold.

Another subtask involved the production of a lower redox potential form of the cytochrome domain in CDH to increase the open circuit potential of the developed BFCs. For this purpose 13 positions in the primary and secondary amino acid shell around heme *b* cofactor of the cytochrome domain were targeted by site-directed mutagenesis. The rationale was to (i) introduce a covalent bond to the cofactor to change the *b*-type heme into a *c*-type heme, which has a lower redox potential, or (ii) to reduce the number of electron withdrawing residues around the heme's tetrapyrrole ring. The obtained results are ambivalent: although several enzyme variants show a lower redox potential (50 to 60 mV vs. NHE) than the wild-type enzyme (100 mV vs. NHE) the IET is also greatly reduced and limits the electron transfer rate. By using the obtained variants, the open circuit potential of the BFC could be increased by a maximum of 50 mV, but the current output would be 10 – 50-fold lower.
On a parallel track, protein engineering of *Hi*CDH was employed to improve the activity on glucose at 5 mM concentration and pH 7. Initially, molecular modelling and docking experiments were performed to obtain a structural model of the enzyme and identify suitable positions for mutagenesis (Fig. 20). The diversity was obtained by site-directed mutagenesis, targeted primary to residues in the vicinity of the active-site, and the resulting variants were screening using two assays: cytochrome *c* and DCPIP as electron acceptors, as measures of DET and MET, respectively (Fig. 21). The best hits from the variant screening were expressed in *Aspergillus oryzae*, purified and characterized to obtain kinetic constants. The optimization of *Hi*CDH resulted in variants with up to 30-fold improved activity on glucose (5 mM), at pH 7, and catalytic rates above 2 s^{-1} (at 5 mM glucose).

Also, some optimization work was done to improve the dehydrogenase activity of *An*GOx, as a measure to improve its activity in MET electrodes. Structure-based mutagenesis with modifications on the active site resulted in improved variants with up to 3-fold higher activity on DCPIP and up to 90% reduced oxidase activity (an unwanted competing reaction). Finally, **GDH from *G. cingulata*** (***Gc*GDH**), which has a high glucose turnover (~500 s^{-1}) at pH 7.4, was employed in electrodes developed for mediated electron transfer (MET). To increase the availability of the enzyme it was

cloned and recombinantly expressed in *P. pastoris* and kinetically characterized (Sygmund et al., 2011b). Additionally, special mutations were introduced to make the enzyme susceptible for covalent attachment to the electrode via linkers to increase electron transfer rates.

In order to obtain a superior enzyme for the second half-reaction (reduction of oxygen), taking place at the cathode (Fig. 22), engineering of two high-redox potential **Lcs from basidiomycetes PM1** and ***Pycnoporus cinnabarinus*** (**PM1Lc** and ***Pc*Lc**, respectively) was undertaken. The initial strategy comprised the replacement of the native signal peptides by the alpha factor preproleader and the joint evolution of the fusion genes to give rise to detectable secretion levels in *S. cerevisiae*. The PM1Lc was subjected to 8 rounds of evolution and screening, engineering a protein mutant (OB-1) with a total laccase activity improvement of 34,000-fold over the parent type (8 mg/L of secreted protein) (Figure 23). The OB-1 mutant harbored mutations V162A, H208Y, S224G, A239P, D281E, S426N and A461T in the mature protein whereas V[α10]D, N[α23]K and A[α87]T occurred at the preproleader. OB-1 was fairly active and stable in terms of temperature (T_{50} = 73ºC), pH profile and the presence of co-solvents. The *Pc*Lc evolution was carried out in the presence of natural and artificial redox mediators enhancing the secretion levels 40-fold along with a 14-fold increase in k_{cat}. The evolved preproleaders were useful for the secretion of native laccases in yeast and constituted a valuable tool for further protein engineering. The evolved *Pc*Lc was also highly secreted by other heterologous host (*Aspergillus niger*) at levels as high as 23 mg/L. The evolved *Pc*Lc harbored mutations N208S, R280H, N331D, D341N and P394H in mature protein whereas showed A[α9]D, F[α48]S, S[α58]G, G[α62]R and E[α86]G at the preproleader. PM1Lc and *Pc*Lc evolved laccases were subjected to a chimeragenesis protocol to shuffle the properties of both enzymes finding new variants with novel pH profiles and/or improved thermal stabilities.

The second challenge of evolving these laccases was to improve the activity at neutral pH and in the presence of high concentrations of chloride ions (human blood resistant). The PM1Lc evolved for functional expression and activity (OB-1 mutant) was selected as starting point to tailor a human blood tolerant laccase. A screening protocol based on the use of surrogate blood (blood buffer with similar biochemical composition as blood but in the absence of cells and coagulation agents) was employed to stress enzymes in the presence of chlorides at alkaline pHs. To make a breakdown of the evolved properties several re-screens were incorporated in each generation finding out the individual improvements in terms of inhibition (vs. halides and hydroxides) as well as stability. After four cycles of evolution and semi-rational approaches (including several site- and saturation-mutagenesis experiments in different positions of the OB-1 gene) an ultimate variant (ChU-B mutant) was engineered containing 2 mutations located at the second coordination sphere of the T1 Cu site (F396I and F454G). The evolved mutant was biochemically characterised from two glycoforms with similar features and slight differences in glycosylations degrees (with molecular weights of 60310 and 58052 Da, respectively). Regardless of the isoform, the pH profile was noticeably shifted as main consequence of the directed evolution (even changing the maximum pH for activity vs. phenolic compounds form 4.0 to 5.0). The residual activity of the ChU-B mutant at pH 7.4 (pH of blood) was 7% for ABTS and 23% for DMP. We are not aware about reports of other HRPLs showing activity at pH above 7.0. ChU-B mutant enhanced its I_{50} for chlorides from 169 mM up to 1024 mM. A less pronounced effect was detected for fluorides (which were not targeted for evolution) with a change in the I_{50} from 69 to 109 mM, for parent and ChU-B mutant respectively. In general terms, the ChU-B mutant showed turnovers in blood buffer of 427 and 143 μmol product μmol laccase^{-1} min^{-1}, for DMP and ABTS, respectively. Neither the parent nor other HRPLs tested in our laboratory (e.g. *Trametes hirsuta* Lc) display activity under such conditions. In collaboration with partner 7B, the mutant was preliminarily characterized in terms of electrochemical responses and direct electron transfer has been detected at electrodes in blood buffer. Finally, in collaboration with Mah, the mutant was tested in real human blood and plasma,

showing activity (measured as consumption of oxygen and using ascorbic acid as reducing substrate). This last mutant was over-expressed in *Pichia pastoris* in collaboration with BOKU and supplied to the consortium for different trials (around 25 mg of pure mutant protein was delivered to the consortium in the final meeting). The mutant was successfully tested in the prototype designed during the final workshop, which took place at Bochum, Germany (RUB).

In summary, the results from WP2 provided improved glucose-oxidizing enzymes both for DET (engineered CDHs) and MET (*Gc*GDH and engineered *An*GOx), as well as oxygen-reducing enzymes, viz. laccase variants with high redox potential and activity in blood buffer, for the construction of glucose and oxygen sensitive biosensors, as well as glucose/oxygen BFCs, much superior to the available bioelements at the start of the project.

WP3. Biomodification of the selected 3D electrodes (Mah, AU, RUB, UL, CSIC, ULUND, NUIG, US).

The main objective of WP3 is to investigate, and report on, methods for electronically addressing glucose oxidising and oxygen reducing enzymes (from WP2) in 3D structures (from WP1). The programme was split into two tasks, the first focused on synthesis and characterisation of a range of redox complexes and polymers that can mediate electron transfer between enzymes and electrodes, and the second task focused on screening approaches for modification of 3D electrode surfaces with components (enzyme, and mediator if necessary) to provide preliminary results on enzyme electrode signal, and signal stability, as a precursor to further tests on biosensor and biopower device operation in WP4.

(i) Generation and characterisation of redox polymers (RUB and NUIG)

Redox complexes, and redox polymers, are used as components of enzyme electrodes in biosensor and biopower devices to enable efficient mediated electron transfer (MET) between enzyme and electrode (electronic wiring of enzyme). A robotic synthesiser system, and/or combinatorial parallel synthesis, using a range of monomeric components (RUB, Fig. 24, Table 1) and polypyridyl ligands (NUIG, Table 2) provided for polymer and redox complex libraries, as presented in Fig. 6. Combination, through parallel synthesis, of elements from the two libraries were then used to prepare a range of redox polymers with a diversity of redox potential (Tables 3 and 4), and physicochemical properties, that could be tailored for the application desired, such as redox enzyme active site potential or immobilization approach. Preliminary characterisation of the polymers, the redox complexes and the redox polymers enabled reporting of the polymer composition (Table 1) and redox complex/polymer potential ($Os^{2+/3+}$ transition, Tables 2-4).

Initial testing of enzyme electrodes prepared using co-immobilisation of redox polymers with model enzymes focused on simple physisorption onto solid (carbon) electrodes and evaluation of the bioelectrocatalytic currents for substrate oxidation (for sugar-oxidising enzymes) or reduction (for oxygenase enzymes). For example RUB have characterised the response for bioelectrocatalytic reduction of oxygen in thin films of selected redox polymers co-immobilised with the *Trametes hirsute* laccase as a function of enzyme loading, shown in Figure 25.

NUIG investigated glucose oxidation by thin films of redox polymer co-immobilised on graphite with glucose oxidase in different ratios, using different crosslinking agents in the presence and absence of added carbon nanotubes (CNT), with results shown in Fig. 26.

(ii) Screening for various procedures for modification/activation of electrode surfaces for facilitating immobilisation/ET with biocomponents and/or mediators

Four types of 3D-nanostructures were fabricated in WP1: (i) CMP, (ii) NMPSi and NMPSiT, (iii) HTGCNT, and (iv) OAN. Work on NMPSi and NMPSiT was not pursued as these electrodes were not sufficiently stable (silicate materials) or did not provide the performance needed (silicon electrodes). These materials were replaced with porous gold modified electrodes which were shown to provide high surface areas (WP1).

Detailed protocols about biomodification procedures for selected 3D-nanostructures were developed and presented in deliverable 3.2, with a brief summary below.

(a) Modification of 3D-porous gold electrodes with cytochrome c and subsequently with redox polymer I/GOx established the high surface area presented by these surfaces (28-fold surface roughness) and resulted in substantial current density for glucose oxidation, as shown in Fig. 27, albeit at high potentials.

(b) Covalent attachment of laccase onto HTGCNT (CSIC/RUB) or gold (CSIC) provided catalytic currents for O_2 reduction, with a maximum current observed by DET of 1.5 mA/cm^2 at +0.2 V vs. Ag/AgCl.

(c) Functionalization of the HTGCNT surfaces with carboxyl groups was carried out by adsorption of 1-pyrenehexanoic acid (RUB) via π-π interaction to further promote physical adsorption in a correct orientation of biomolecules (BOx, Lc). Onset of the catalytic oxygen reduction at approximately +0.7 V was observed for laccase adsorbed onto modified HTGCNT and the high catalytic current densities in the absence of redox mediator measured indicate adsorption over favours orientation with the Cu T1 redox site facing the electrode.

(d) Nanostructures fabricated using the **glancing angle deposition** (**GLAD**) technique were used to adsorb GOx with significantly more binding of enzyme, compared to flat surfaces.

(e) Three-dimensional AuNP enzyme electrodes were fabricated on Au-disk electrode by solution casting of previously prepared and characterised AuNPs followed by deposition and mixing of enzymes (CDH or BOx) to provide 3-D reaction volume for bioelectrocatalysis.

Finally, as part of WP3 flexible surface attachment chemistry (US) for carbon surfaces was developed using a high-yielding maleimide coupling of enzyme to pre-treated carbon surfaces, as reported on in deliverable 3.3.

WP4. Characterisation and optimisation of microscale 3-D biodevices (AU, RUB, UL, CSIC, ULUND, NUIG, US).

The aim of WP4 represented the evaluation of the optimum combinations of biocatalysts (provided from WP2), mediators (provided from WP3), electrode supports (provided from WP1) and immobilization approaches (provided also from WP3). As a matter of fact, the progress within WP4 benefited from the concepts and delivered materials from WP1-3, with the initial aim to fulfill the specified technical criteria agreed achieved in deliverables D4.1-D4.5. Based on the fulfillment of D4.1-5 deliverables, in terms of current densities and operational onset potentials, the main focus of WP4 was directed towards reaching the power generation conditions required by the electronic design of the sensing device, and to secure its operation with satisfactory stability under physiological conditions in terms of substrate concentration, pH, halide concentration, as stipulated within WP5. The power generation conditions, required for further experiments within WP5, were

set by the consortium to an operational cell potential of 600 mV and a minimum generated current of 40 μA. This had to be provided by fully integrated-operational BFCs combinations, for which the corresponding bioanodes and biocathodes relies on enzymatic concepts established by the consortium.

As a final testing of optimum combinations of bioanodes/biocathodes operating at pH 7 and in artificial serum medium, a join-experimental session was organized in April 2012 at RUB and included all the partners involved in the project. The final conclusive experiments (belonging to WP5) in Bochum demonstrated the feasibility of a self-powered device, operating under oxygen and glucose, and capable of sensing the concentrations of oxygen and glucose in an artificial serum, and further to wirelessly transfer the recorded signal to an external receiver.

A large number of various configurations of bioanodes and biocathodes were tested for construction of biofuel cells, by each individual partner, as well as within cooperations based on short visits and exchanges. Among all those trials, the following examples are meritorious to be mentioned here, and which are structured in accordance with projects Tasks 1-5:

Task 1. Extensive electrochemical characterisation, optimization, and selection of 3D-nanobiodevices based on DET reactions.

Bioanodes

ULUND presented two protocols for fabrication of a bioanode based on modification of gold electrodes with (i) AuNPs and (ii) CNTs. *Ct*CDH developed by BOKU was selected as the bioelement. The choice of *Ct*CDH as main tested enzyme was because it is known to be the best glucose oxidising CDH at neutral pH, combined with its good DET properties at the surfaces of the electrodes.

AuNPs surface was modified by a mixture of thiolic **self-assembled monolayer** (**SAM**) containing 4-aminothiophenol and 4-aminobenzoic acid. *Ct*CDH was further cross-linked between the amine groups on the surface of the electrode and with the lysine residues on the surface of CDH using glutaraldehyde as cross-linker through the formation of imine bonds. The covalent attachment produces a stable platform for the enzyme in terms of stability and the linkage is flexible enough to allow possible movements of the enzyme. The electrocatalytic activity found on these type non-nanomodified electrodes for the oxidation of sugars was low and with no real applications for biofuel cells.

Covalent coupling of CDH onto diazonium salt activated SWCNT on 3D-microarray carbon electrodes

A three-dimensional microstructured carbon electrode array was fabricated and characterised by ULUND. The 3D-microarray carbon electrode (Fig. 28) was further the electric and physical support for deposition diazonium salt activated SWCNT, onto which CDH was covalently attached. Biocatalytic current in presence of 5 mM lactose shown an oxidative onset potential of -200 mV vs. $Ag|AgCl_{sat}$, a value that suggests DET from the CYT_{CDH} to the electrode (Fig. 29). This low potential value obtained makes the immobilisation procedure suitable for BFC applications where as low potential as possible being desired for a higher **open circuit voltage** (**OCV**). The operational stability *Ct*CDH/SWCNT/3D-micropost was examined in PBS measuring LSV continuously for more than one week. For 5 mM glucose containing buffer approximately 10% drop of power density was observed after continuous operation for 9 days. This SWCNT activated protocol was also successful applied for other CDH mutants with enhanced glucose oxidation properties, produced from *Hi*CDH and *Ct*CDH by NZ and BOKU, respectively. Excellent DET properties and interesting effect of $[Ca^{2+}]$ or **polyethyleneimine** (**PEI**) onto AuNPs were also demonstrated by ULUND for other CDH enzymes, or using PDH or GDH.

RUB demonstrated that simply physical adsorption of **CDH from *Trametes villosa*** (***Tv*CDH**) onto 3D-HTGCNT electrode (produced at RUB) shows a high current density of ~ 4 $mA \cdot cm^{-2}$ (electrode area of 1 cm^2) at +200 mV and in presence of 10 mM lactose (Fig. 30), which implicitly represents a highly efficient DET. Meritorious to emphasise the onset potential at approximately -300 mV (vs. Ag|AgCl), which is very close to the known formal potential of the FAD cofactor, which represents a very strong advantage for BFC application.

Biocathodes

Direct electron transfer was proven as a facile approach for fabrication of biocathodes, as demonstrated by various protocols, which shown excellent biocatalytic properties based on oxygen reduction at various bioelements, such as Lcs or BOxs, wither as wild type or mutants. CSIC in collaboration with RUB shown that utilisation of 3D-hierarchical carbon electrode (produced at RUB) is an ideal supporting platform for immobilisation of *Th*Lc derivates as promoters for specific and stable orientation onto CNT/CMF structure. The electrocatalytic activity of *Th*Lc electrode for O_2 reduction was measured by CV with the 3D-biocathode adapted to an electrode rotator (Fig. 31). The onset of the catalytic activity at 0.7 V and the high catalytic current densities in absence of redox mediator measured indicate that the immobilisation strategy favours orientation of the Lc with its Cu-T1 redox site facing the electrode. In addition, the high surface area of the 3D-electrode allows a high coverage of enzyme on the electrode and its carbon nanotube network enhances the rate of DET. Because of this, the catalytic current density is rate-limited by the mass transfer of O_2 (Fig. 31). The plateau current densities measured are approximately -1.5 mA/cm^2 and -0.6 mA/cm^2 with O_2-saturated and air-saturated solutions, respectively. Moreover, these current densities are reached at quite high potentials as shown in Fig. 31, which is a positive feature for its application as a BFC cathode.

Covalent immobilisation of *Th*Lc onto low density graphite electrode modified with gold nanoparticles (DET-CSIC) was shown by CSIC, using grafting with 4-aminophenyl groups. Afterwards, AuNPs of average size 7 nm were covalently linked to the functionalised electrode, resulting in a large coverage of AuNPs within the porous structure of the graphite. Subsequently, the exposed surface of AuNPs was modified with a mixed monolayer of 4-aminophenyl and 6-mercapto-1-hexanol groups for the covalent attachment of laccase molecules (Fig. 32). The onset of the catalytic activity at approximately 0.7 V (vs. Ag/AgCl) and the high catalytic current densities in absence of redox mediator measured indicate that the enzyme covalently bound to the AuNP-modified electrode favours orientation of *Th*Lc with its Cu T1 redox site facing the electrode (Fig. 31). The porous surface of the low density graphite electrode allows a high coverage of enzyme on the electrode and the monolayer of AuNPs enhances the rate of DET. Therefore, high current densities of O_2 reduction are measured (1.14 mA/cm^2 and 0.46 mA/cm^2 at + 0.2 V with O_2-saturated and air-saturated solutions, respectively).

US had also demonstrated another successful procedure for covalent immobilization of *Th*Lc onto 3D-hierarchical carbon nanotubes electrodes via modification with anthraquinone derivatives. The coverage of the HTGCNT electrode with 100% correct orientation of the enzyme for efficient DET is proven by the fact that addition of mediator molecule do not contribute to any further enhancement of biocatalytic current via mediated electron transfer. CVs show that biocatalytic reduction of O_2 started at known potential from literature (+650 mV vs. Ag|AgCl) and leads to a current density of approximately 250 $\mu A/cm^2$. The experiments at rotating disk electrode (Fig. 33) show the fact that the current density is limited by the mass transfer of O_2 within the biocatalytic nano-domains onto the electrode. The current densities drop slowly with overall decrease by 21.2% over 168 hours (7 days). More significant decrease occurs in first 48 h (10.7%) followed by stabilised response.

Also, based on DET reactions, Mah reported the assembly and characterisation of a high potential, stable, mediator-less and cofactor free biocathode based on a fungal Lc, adsorbed on highly

dispersed carbonaceous materials. The carbonaceous material BM-4 was chosen to design efficient and stable biocatalysts for the production of a 'floating' air diffusion Lc-based biocathode. The current density of oxygen reduction at the motionless biocathode in a quiet, air saturated citrate buffer (100 mM, pH 4.5, 23 °C) reached values as high as 0.3 mA cm^{-2} already at 0.7 V versus NHE.
UL demonstrated well defined mediatorless bioelectrocatalytic reduction of O_2 with high current densities of 0.8 mA cm^{-2}, obtained on nanoporous gold electrodes modified with ***Myrothecium verrucaria*** **BOx** (***Mv*BOx**). A stable faradaic response was observed when the enzyme modified electrode was coated with a specifically designed electrodeposition polymer layer. The response of the enzyme electrode was only slightly inhibited by the addition of F..

Task 2. Screening of enzymes selected as good candidates for MET-based devices, in-depth characterisation and optimisation of individual glucose oxidizing and oxygen reducing devices based on selected enzymes/surfaces/redox polymers combinations operating in MET mode.

Bioanode
Extensive optimisations for an efficient MET were investigated in terms of involved bioelements, such as several types of CDH (wt/recombinant/FAD-only), FAD-dependent FDH (**FAD-GDH**), **pyranose dehydrogenase** (**PDH**); electrode structures, such as graphite electrodes (ULUND), HTGCNT (RUB), mesoporous Au-electrodes (UL); "redox polymers" containing various Os-complexes with different formal potential or carrying phenothiazine derivatives as $2e^-$ relay.
NUIG has shown an increase of electronic conductivity within [Os(2,2'-bipyridine)$_2$(polyvinylimidazole)Cl]$^+$ redox hydrogel by co-immobilization of *An*GOx in presence of MWCNT and using a range of crosslinking agents. Amperometric current densities of 2.45 mA cm^{-2} and 4.51 mA cm^{-2} were obtained for electrodes without and with MWCNT, respectively, in 100 mM glucose, 37°C, 50 mM 7.4 pH PBS (150 mM NaCl), stirred at 150 rpm. Despite of high current densities obtained, the high redox potential of the redox polymer mediator (0.25 V) disqualifies in principle its usage for BFC application.
The various new **GDH from *Glomerella cingulata*** (***Gc*GDH**), or recombinant species, produced, characterised, and provided by BOKU, were electrochemically characterised by ULUND using various osmium redox polymers synthesized by NUIG (Fig. 34). The highest current density of 493 µ A cm^{-2} for 30 mM glucose was generated, and it is applicable as a glucose biosensor applications with preferable features of being insensitive to O_2 and with a high specificity, selectivity, and catalytic efficiency comparable with that of commercially available *An*GOx.
In another approach (ULUND) two C-1 oxidising oxidases, i.e., *Mt*CDH and *Gc*GDH were combined with the C-2 and C-3 sugars oxidising enzyme, **PDH from *Agaricus meleagris*** (***Am*PDH**). This last approach, where the enzymes are combined, produces more efficient power output per sugar molecule. Up to six electrons can be extracted from a single glucose molecule.
In order to circumvent the obvious limitations of Os-containing redox polymers in respect to too high formal potentials for a good bioanode candidate, a new concept of redox hydrogel was proposed, based on a two electrons acceptor containing polymer, such as phenothiazine as redox relay (RUB). The concept was successfully tested for CDH (ULUND and RUB) and it was applied for the BFC integration test within WP5.

Biocathode
Biocatalytic reduction of O_2 was investigated by NUIG using *Mv*BOx co-immobilized within a [Os(2,2'-bipyridine)$_2$(polyvinylimidazole)Cl]$^+$ redox hydrogel on glassy carbon electrodes and the current density was studied in presence and in absence of MWCNT, using a diepoxide crosslinking agent. Amperometric current densities of 0.7 mA cm^{-2} and 1.5 mA cm^{-2} were obtained for

electrodes without and with MWCNT, respectively, under oxygen purging and at physiological conditions 37°C, 50 mM 7.4 pH PBS (150 mM NaCl).

Extensive bioelectrochemistry studies carried out by RUB demonstrated that various Os-polymers might pose interesting extrinsic properties for *Th*Lc, such as resistance to chloride inhibition of the enzyme once it is entrapped in a specific Os-polymer film.
As was also presented for DET, UL used the mesoporous gold electrode, fabricated in their group, for the entrapment of *Mv*BOx within $Os(2,2'\text{-bpy})_2(PVI)Cl$ polymeric film (formal potential of +228 mV vs. Ag|AgCl), stabilized via cross-linking with **polyethyleneglycol diglycidylether** (**PEGDGE**). The diffusion limited current densitiesobserved arise from O_2 diffusionto the enzyme.

Task 3. Testing performances of biofuel cells designed from the optimized biocathodes and bioanodes.

BFC schemes
Various techniques (linear sweep voltammetry, pulse voltammetry, CV, or **open circuit potential** technique (**OCV**)) as well as different experimental setups were used for studying and monitoring individual bioanode/biocathode combinations for integration within a fully functional BFC. Specifically, one (Fig. 9) and two compartment based BFCs were designed and studied (Figs. 2 and 35).
As an example of a designed, investigated and published BFC, it can be mentioned the work of Mah and ULUND. In collaborative studies these partners fabricated and characterized a gold-nanoparticle (AuNP)-based mediatorless sugar/oxygen biofuel cell (BFC) operating in neutral sugar-containing buffers and human physiological fluids, such as blood and plasma. First, *Ct*CDH and *Mv*BOx, used as anodic and cathodic bioelements, respectively, were immobilised on gold electrodes modified with 20 nm AuNPs. Second, the *Ct*CDH/AuNP-based bioanode was combined with the *Mv*BOx/AuNP-based biocathode, for a functional BFC. The following characteristics of the mediator-, separator- and membrane-less, miniature BFC were obtained: in phosphate buffer; an open-circuit voltage of 0.68 V, a maximum power density of 15 $\mu W\ cm^{-2}$ at a cell voltage of 0.52 V and in human blood; an open-circuit voltage of 0.65 V, a maximum power density of 3 $\mu W\ cm^{-2}$ at a cell voltage of 0.45 V, respectively (Fig. 36).
Several other examples were studied and their results are under process of publication.

Task 4. Fabrication of selective and stable glucose and oxygen biosensors.

Glucose sensor was constructed by ULUND using wild type *Ct*CDH adsorbed on screen printed electrodes and stabilized using glutharaldehyde as crosslinker. The calibration plots of the sensor towards glucose are presented in Fig. 37.
Another biosensor for glucose was developed using two recombinant *Hi*CDH, showing large spectra of variation of substrate specificity among different oligosaccharides.

An oxygen biosensor was fabricated at CSIC by covalent immobilization of *Th*Lc onto functionalised HTGCNT from RUB. CSIC developed methods for the fictionalisation of the carbon electrode surface, by electrochemical reduction of 4-nitrobenzene diazonium salt, resulting in a covalent attachment of the enzyme and the electrochemical characterization of O_2 biosensor. Specifically, the sensitivity of the laccase electrode towards the O_2 substrate was measured by chronoamperometry at +0.2 V *vs.* Ag/AgCl (3M) in an electrochemical cell with acetate buffer pH 4.2 purged with N_2, thermostated at 27ºC, and a electrode rotation of 250 rpm. Aliquots of buffer saturated with pure O_2 at room temperature were added to the solution and a transient decrease of the current was detected due to the immobilised Lc activity and direct electron transfer between

enzyme and electrode (Figure 38). The nanostructured electrode allows a high loading of enzyme on the electrode, and the Lc immobilization method together with the carbon nanotube network of the electrodes optimizes the direct electron transfer between the components of the biosensor. In Fig. 39 linear response of the biosensor towards low concentrations of oxygen is demonstrated. A detection limit of 0.7 ± 0.2 μM and a sensitivity of 8.8 ± 0.6 A cm^{-2} M^{-1} for O_2 has been determined from three replicate experiments. The inset of Figure 39 shows that the linear range of the O_2 biosensor is up to 225 μM. However, the concentration of O_2 in air-saturated aqueous solutions is not above the upper limit of the linear response of the biosensor. Therefore, the linear range of the developed O_2 biosensor is satisfactory.

Task 5. Analysis of the performances of enzyme-based 3D biodevices.

Basic properties (current densities, operating voltages, etc) of designed biocathodes and bioanodes are summarised in Fig. 40. Overall interpreting the performances and limitations of various bioanode and biocathode electrodes, as well as their functional compatibility in terms of pH operational range or operational stability, one can summarise the following:
(i) Biocathodes, despite of limited concentration of O_2 in air-saturated solutions (200-300 μM), demonstrated that those conditions of high operational potential, as well as required current densities can easily be achieved. The only ultimate limitation of the performance of a biocathode is remaining, as demonstrated above, the intrinsic limit of diffusion of O_2 toward bioelectrocatalytic sites on the surface of electrode.
(ii) Bioanodes has shown that an extensive 3D-structure for increasing the loading of the bioelement does not necessarily contribute to a dramatic increase of the current densities. A first hand explanation is attributed to the molecular size of the anode substrates (comparison between glucose/ monosaccharide and lactose/ disaccharide) and their much lower diffusion coefficients, at least in comparison to O_2. A second explanation in the same direction is given by inclusion of various polymeric matrixes which implicitly induce a further restriction of the mass transport over all the highly loaded catalytic volume. Another major milestone is represented by their onset operational potentials, somehow too high for a routine protocol for fabricating the bioanodes. A future solution is represented by the proper exploitation of other redox mediators (e.g. phenothiazine) or specific engineered orientation of the enzymes onto the electrode surface in order to address directly those thermodynamic efficient catalytic cofactors of the enzymes (e.g. FAD of CDH and exclusion of electronic involvement of heme-cofactor), without compromising any kinetic properties of the optimised catalytic process.

WP5. Fabrication, characterisation, and tests of microscale self-contained biodevices for biomedical application (Mah, NS, ULUND).

The WP5 contained 3 main tasks, which were fulfilled as described below.

Task 1. Fabrication and optimisation of transmitting/transducer system with incorporated operational unit based on CC2430 microchip
At the beginning of the project some Partners (e.g. Mah, RUB, ULUND) were able to provide BFCs operating at 0.5 V or even less and providing few μW/cm^2 power. These values were obtained from studies of not-optimised DET and MET based BFCs, which were fabricated based on available bioelements. The biodevices were characterised in simple buffer solutions and human physiological fluids, e.g., human serum. At the end of the project bioevices generating voltage of 0.6-0.8 V with few tens or even hundred μW/cm^2 power densities were designed. The performance of biodevices was tested in simple buffer solutions and human physiological fluids, e.g., human blood, plasma, serum, and saliva.

One of the major tasks of NS was to address incompatible difference of voltage and power between the data transmitting systems and even optimised BFCs. First, an energy-harvesting module was designed. One of the tasks for the energy-harvesting module was to step up the low voltage the fuel cell delivers to a usable voltage for standard electronics. State of the art low power electronics (commercial available) still need quite a lot of energy, e.g. 90 000 μW for radio transmission and 2 000 - 20 000 μW for sampling. Thus, the energy-harvesting module also was designed to store energy and to control the activation of the standard electronics. This was necessary as standard electronics also draws too much power in "stand-by mode". After the energy-harvesting module had stored enough energy to sample data and transmit one data package the radio module was activated from a control circuit via a switch (Fig. 41). The CC2530 chip and measuring electronics was thus activated from the energy-harvesting module. The CC2530 has an integrated ADC, which was used to sample glucose and oxygen values from the measurement electronics. The data was directly transmitted to the receiver which was turned on all the time for receiving data. When the radio module had transmitted the information a signal was sent to the energy-harvesting module which then turned off the "standard" electronics (radio and measurement electronics, see Fig. 41).
To integrate glucose sensing with the data transmission system a simple potentiostat was incorporated into the electronic device (Fig. 42). One of the biofuel cell electrodes serves as a counter and reference electrode. To minimise errors in glucose measurement, digital and analog integration of the sensor signal were used and optimised. As was planned in DoW the errors did not exceed 10% of the mean value from the bioanalyte signal.
Embedded software required to control the developed sensor system was developed. The main purpose of this software was to start up needed modules, sample sensor data and transmit the data safely to a receiving unit. This sequence of tasks should be as fast as possible to save power. The timing of wake up, sample, transmit data and sleep can be seen on the green curve in Fig 43, which represents current consumption. Total duration achieved was 4.6 ms, whereof 3 ms was with radio transmitter activated. It should be noted that when the radio unit had completed the given task, a control signal was sent to the energy harvest module to shut down the switch providing power to the measurement electronics and radio transmitter. Thus the charging for next sample could commence immediately after finalising transmission. The transmitted package via the transmitter in the sensor was sent unsynchronised to the receiver to preserve energy and keep the sensor uptime low. Thus software for receiver had to operate continuously and wait for the next transmitted package from the receiver. However, this did not present a difficulty as the receiver connected to a computer did not consume more than 40 mA. When a package was received by the receiving radio the package was sent to an USB module, which was connected to the computer (Fig 44).

Task 2. Fabrication of wireless devices for glucose or oxygen monitoring.
Both glucose and oxygen sensitive wireless self-powered devices were fabricated as described in deliverables 5.5 and 5.6. Specifically, all different parts of a wireless self-powered biodevice, which were developed by Partners during the project, i.e. the electronic unit (containing energy harvesting module, potentiostat for a glucose or oxygen biosensor, and wireless communicating device, i.e. radio module), glucose or oxygen sensitive biosensor, and a sugar/oxygen BFC, were combined together into a functional unit (Fig. 2). The general idea for electronics was to have the radio module turned off and when enough energy had been harvested by the energy harvesting module then wake up the radio module and the task at hand would then be: 1) to measure and sample data, 2) to establish a paired connection to a receiving radio base, 3) to send the measurement data via the radio, and finally, when the message has been transmitted, 4) to signal to the energy harvesting module to turn off the power supply and begin to store energy again. The receiver is then connected to a computer and is actively listening to new messages from the wireless sensor. When a message is received the data is extracted, stored, and displayed together with the time stamp for the data. These methods were adopted, implemented, and tested. The general scheme of the system setup can

be seen in Fig. 45. For preliminary studies of developed demonstrators for glucose and oxygen biosensors, a single cell battery was used instead of BFCs (Fig. 46). As glucose or oxygen sensitive biosensors AuNPs modified gold microwires (100 μm) with immobilised *Ct*CDH or *Mv*BOx were used. The performed preliminary tests revealed some limitations of the sensor electronics in the case of glucose sensing. Indeed, a new design for a glucose sensitive biodevice was developed. The old sensor electronics was primary developed for oxygen measurement, but with glucose the reference electrode is instead the anode. Thus, the negative power supply converter was not needed and the sensor electronics was reduced to a simple potentiostat meter with single power supply, see Fig. 47.
Thus, both prototypes to measure glucose and oxygen were fabricated and delivered to the Consortium. Some photos of a self-contained biodevice can be seen in Fig. 2.

Task 3. Device testing.
In the frame of this task separate units of self-contained biodevices, *i.e.* electronic units, biocathodes, bioanodes, and complete BFCs, as well as two self-powered wireless biodevices were investigated including biodevice tests in simple buffer solutions and complex biological fluids, such as blood, plasma, serum, and saliva. Prior to these tests, the particular concentrations of two bioanalytes, viz. glucose and oxygen, in biological matrices was accurately measured using commonly used techniques (Fig. 8), to enable correlation studies between the different devices to be performed.
Firstly, designed glucose oxidising and oxygen reducing biomodified electrodes were tested under cell culture conditions (Fig. 10) to investigate biocompatibility of the developed bioelectrocatalytic systems. For this purpose, oxygen reducing and glucose oxidising biodevices were designed in cell culture plates containing a permeable membrane as a bottom (Fig. 10.1). The system was created by using disposable electrode arrays, 8W2x1E (Applied Biophysics, USA) which were modified prior to investigation to be used as biodevices. Each array contained eight wells with two planar gold electrodes each (Fig. 10.1). The construction and the performance of the biodevices were optimised for several days monitoring of both bioanalytes in cell culturing condition. It was shown that catalytically inactive elements of biodevices, e.g. non-biomodified nanostructured surfaces based on CNTs, do not affect attachment and growth of cells on the surfaces (Fig. 10.2). However, the introduction of biocatalysts, e.g., GOx or BOx enzymes, made surfaces strongly toxic even when biodevices are not electrically connected (Fig. 10.2). The effect of GOx can be easily explained by the generation of hydrogen peroxide at GOx modified surfaces since both substrates of the enzyme are present in the solution, glucose and oxygen. In case of BOD the result cannot be explained by BOx catalytic reaction since in the absence of electron donors (without applied potential) the enzyme does not function. Further investigations are needed to understand the cell toxicity of certain nanostructured surfaces.
Secondly, the most successful constructions from WP4 were investigated in detail in biological fluids, such as blood, plasma, serum, and saliva, and limitations in their performances were studied and summarised. This included the tests of separate glucose oxidising (glucose sensitive biosensors and bioanodes) and oxygen reducing (oxygen sensitive biosensors and biocathodes) 3D nanobiodevices, as well as complete glucose/oxygen BFCs. It was shown that in simple air saturated buffer solutions bioanodes usually limited the performances of BFCs. However, when biodevice were investigated in complex air saturated physiological fluids significant decrease in biocathode performances was observed. Indeed, in real implanted situations, when free O_2 concentration is much lower than 0.25 mM, BFCs might be limited by oxygen diffusion to the electrode nanostructured surfaces of biodevices.
Finally, two prototypes for monitoring of glucose and oxygen concentrations were tested using a battery instead of BFCs. From the very beginning of these tests the procedure to calibrate both systems was developed as described in deliverables 5.5 and 5.6. After the calibration of systems, the

biodevices were tested. Specifically, the subsequent addition of bioanalytes in physiologically relevant concentrations (5 mM glucose or 0.25 mM oxygen) to the electrochemical cell resulted in the wirelessly measured signal, which was three or more times higher compared to the background value (Fig. 48). To conclude, developed wireless electronic and operational units showed very stable and reliable wirelessly monitored signals. The next step was to perform analogous experiments powering the system with a BFC developed by the Consortium. This was done during the final meeting of the Consortium in Bochum (RUB University), Germany. A joint measurement session (5 working days) was organised with several tasks including the final test of two wireless self-powered biodevices, viz. glucose and oxygen sensitive self-contained biodevices (Fig. 2). Two compartment BFCs were built using several different (mediator-based and mediator-less) bioanodes and biocathodes because of two main reasons, viz. (i) in order to achieve both current and voltage required for electronics, viz. ≥44 μA and ≥0.57 V and (ii) in order to use all developed bioelectrodes to equalise contribution of all project partners. The following maximal parameters for the combined BFC were obtained: open circuit voltage of 0.73 V, 58 μA at 0.67 V operating voltage. To increase the power of the BFC, lactose and oxygen at high concentrations, e.g. 10 mM and 0.25 mM, were used as biofuel and biooxidant in the anodic and cathodic compartments of the biodevice. Since lactose and oxygen are required to produce electric power their concentrations could not be significantly decreased during the tests.

The procedure to calibrate systems was exploited and operating voltage in the system was monitored by the external voltmeter (Fig. 2A, yellow box). Variation of bioanalytes concentrations resulted in corresponding variation of wireless signals (Fig. 48). Moreover, wireless signals from sugar and oxygen sensitive biodevices powered by BFC have been measured successfully for a long time, 1-2 hours. During this time several tens of packages of information were received wirelessly by the receiver (Fig. 2B), which was located 4 meters away from tested biodevices (Fig. 2A).

Literature

Camarero S., Cañas A., Martínez M.J., Martínez A., Ballesteros A., Plou F.J., Record E., Asther M. and Alcalde M. (2010) Patent: WO/2010/058057.

Camarero S., Pardo I., Cañas A.I., Molina P., Record E., Martínez A.T., Martínez M.J., Alcalde M. (2012) Appl. Environ. Microbiol. 78, 1370-1384.

Harreither W., Sygmund C., Augustin M., Narciso M., Rabinovich M.L., Gorton G., Haltrich D., Ludwig R. (2011) Appl. Environ. Microbiol. 77, 1804-1815.

Harreither W., Nicholls P., Sygmund C., Gorton L., Ludwig R. (2012) Langmuir 28, 6714-6723.

Mate D., Garcia B., Alcalde M. (2010) Chemistry and Biology 17, 1030-1041.

Mate D., Valdivieso M., Fernández L., Alcalde M. (2011) Patent: WO/2011/144784.

Sayut DJ and Sun L (2010) Chemistry and Biology 17, 918-920.

Sygmund C., Klausberger M., Felice A., Ludwig R. (2011) Microbiology 157, 3203-3212.

Sygmund C., Staudigl P., Klausberger M., Pinotsis N., Djinovic-Carugo K., Gorton L., Haltrich D., Ludwig R. (2011) Microb. Cell Fact. 10, 106.

Wang C., Taherabadi L., Jia G., Madou M., Yeh Y., Dunn B. (2004) Electrochem. Solid State Lett. 7, A435.

Xu H., Malladi K., Wang C., Kulinsky L.., Songb M., Madoua M. (2007) Biosens. Bioelectron. 23, 1637.

4. Potential impacts

The multidisciplinary "3D-nanobiodevice" consortium addressed several highly challenging, multi-industrial, and interdisciplinary objectives. To solve these "3D-nanobiodevice" brought together leading scientists in the nanobiotechnology field specialising in investigations on enzyme-nanostructure interactions (e.g., enzyme-nanoparticle), integration of nanostructures and enzymes into 3D catalytic and electrically conducting structures for BFC applications and diagnostics. Nanostructures and biocatalysts (redox enzymes), knowledge on their interactions, design of BFCs using nanobiocomposites, and development of modern low voltage miniature electronics were some of the many outcomes of this Consortium, outcomes that could not be achieved at any national level. Only European cooperation provided an opportunity to develop 3D nanobiostructure-based bio-electro-catalytic elements, which have a quality required to produce competitive self-contained wireless devices and evaluate these in biomedical application. One of our aims was to put the major fundamental goals of the project "a better understanding of the interactions between bioelements and 3D nanostructures and fundamental principles for exploiting and developing electro-conducting nanoarchitectures to assemble highly efficient 3D bioelectrocatalytic structures" into a practical test by assembling a device consisting of BFC, biosensor, and wireless radio transmitter and evaluating its performance in biological fluids. This was a practical step beyond the state-of-the-art.

A convergence across industries and interdisciplinary studies resulted in breakthrough applications at the interfaces of energy and healthcare areas (Fig. 3). The consortium contained two key industrial partners, viz. Novozymes A/S (NZ) and Novosense AB (NS), both of which are eager to pick up the technological progress of the project for future commercialisation.

Novozymes A/S, a world leader in industrial biocatalysts production, is part of NovoNordisk, one of the leading producers of insulin and insulin pumps worldwide. The involvement of Novozymes in this project indicates that the company as a whole (*i.e.*, NovoNordisk) is extremely interested, e.g., in acquiring "3D-nanobiodevice" technology for the development of non-invasive glucose monitoring and wireless actuation of insulin pumps and their commercialisation in the health sector. Additionally, the development of 3D-nanobio-based BFCs is expected to contribute to a breakthrough in the Energy area (see Fig. 3), where Novozymes A/S has identified considerable potential to expand their commercial interests as an enzyme producer.

The second industrial partner of the consortium, Novosense AB, is a young biomedical engineering company, with currently limited commercialisation potential simply because it is small. However, the company is working with wireless medical devices, which was a key issue of "3D-nanobiodevice" project. The company is developing wireless communication protocols to "wire" medical instrumentation to databases at hospitals. This project enabled the company to develop means of minimising energy consumption for wireless transmission, to design an electric energy harvesting block and voltage amplifier, and thus progress the future integration of BFCs and biosensors into new wireless health care facilities. Additionally, the development of methods of integrating wireless medical devices to databases at hospitals has tremendously shortened the time needed to bring self-contained biodevices to the consumer market.

The potential commercial impact of the project is described in the preceding two paragraphs, which comes through direct collaboration with the industrial partners of the project, NS and NZ. However, the impact directions addressed in collaboration with the partners are much more general. More and more healthcare services and operations are conducted at homes and this trend converts healthcare system into a distributed biomedical industry, where biomedical devices are operated by patients or healthy humans. Healthcare innovations are accentuated by terms such as home based healthcare,

mobile healthcare, point of care devices, wireless sensor networks, non-invasive monitoring, wearable and attachable biomedical devices, etc. The expected changes of healthcare systems to some extent can be compared with the changes of financial sector. We use credit cards and decide on credit limits, pay bills over the internet, and take loans without going to the bank. We enjoy financial autonomy. Surrounded by biomedical devices we will decide over our healthcare needs in the future much more than we do today. It is well realised that one of the bottlenecks to the use of distributed biomedical devices is a stable and reliable energy supply. It is hard to accept that we will change batteries in a number of biomedical devices at home every day or even every month. In this project we have been pursuing intensive research to develop and test BFCs as a reliable alternative for powering biomedical devices. We believe that BFCs will become an important power source in new generations of self-contained biomedical devices with self-powering and wireless capabilities. Thus, the progress achieved in this project on the development and combination of BFC with other biomedical devices have a very high impact on innovations promoting the establishment of distributed biomedical industry.

The ultimate goal of the Consortium was to create self-contained miniature biomedical devices possessing wireless communication capabilities for implantable exploitations. Taking into account the world market for biosensors (ca. US$15 billion in 2010 with an annual growth rate of 5%), it is very hard to overestimate the economic effect of this Project related on modern biosensor technologies. Over half of the biosensors produced worldwide are employed in glucose meters. The possible economic effect of the project in terms of projected economic feasibility (Table 5) is based on glucose sensitive devices, both in short-term perspectives (i.e., in 3 years after the end of the project; in the year 2015) and in the long run (i.e., in 10 years after the end of the project, e.g., in the year 2022). Moreover, the total economic effect of the "3D-nanobiodevice" project is even higher because many other devices with possible commercial futures, e.g. different types of potentially implantable BFCs (mediator based and mediator less), electronic transmitter/transducer systems, oxygen sensitive microbiosensors, was also developed by the Consortium. In general, "3D-nanobiodevice" bioelectronic technologies, e.g., preparation of efficient 3D nanobiocatalytic structures or separate units, such as BFCs or biosensors, may provide valuable impact for the Energy sector (BFCs), the environment (waste water treatment), and the development of in vitro diagnostics, whereas designing of microelectronics and modern software might accelerate the development of the IT sector.

According to the World Diabetes Market report, diabetes affects approximately 200 million people worldwide and is expected to increase to 300 million diabetics by 2025. In many developed countries (e.g., USA, European Union) more than 5% of the population suffer from diabetes. It is the 6th most common cause of death as recorded on US death certificates. With a diabetes epidemic underway, there exists strong growth opportunities for diabetes management tools, such as glucose meters. Over the years, glucose-monitoring meters have undergone a sea change, with recent entries featuring wireless and sensor technologies. Sales in United States, the largest market for glucose biosensors, are expected to reach US$1.3 billion by the end of 2012. The data presented in Table 5 are based on the prediction that less-complicated devices produced by the consortium, i.e. microbiosensors, will pass clinical trials, be commercialised and account for less than 1% of the total market existing for glucose sensitive biosensors in 2015. Only in 2022 one can expect real commercialisation of wireless implantable self-powered biodevices for continuous glucose monitoring.

It is very hard to estimate the long-term perspectives for devices due to the existence of many different and unpredictable factors affecting their sales. However, taking into account the 5% per annum growth rate on the biosensor market as well as a robust management strategy, one can

expect 2.5 times increased sales for microbiosensors in 2022 along with appearance of self-contained implantable biodevices for glucose monitoring on the European market, which will replace simple microbiosensors.

A long-term objective of the Project is to facilitate development of environmentally and body-friendly nanotechnologies for biomedical applications. Profound fundamental knowledge gathered during the project will provide the necessary knowledge for medical exploitation of 3D nanobiostructures as a basis for self-contained wireless biodevices consisting of a BFC, (bio)sensor(s), and a miniature signal transmitter system. The benefits to the society gained from the project can be foreseen as an acceleration of exploitation of knowledge-based products for sustainable innovations of the biomedical industry sector. The project facilitated the integration of biosensors, chips, and BFCs into integrated biomedical devices. It can be predicted that the developed technology will be used to improve quality of life and increase safety in case of widely occurring chronic diseases, when miniaturisation of self-contained and potentially implantable 3D nanobiostructure based devices is done. In the long-run, 3D nanobiostructure-based elements will be essential for constructing devices to be used for neuron/nerve stimulations and compensation of human disabilities.

Additionally, touching on the environmentally and body-friendly development of power sources in form of BFCs, the following can be emphasised. A great deal of the project has been focussed on enhancing BFC performance based on DET reactions between the enzymes and nanostructures. The realisation of DET principle allows more facile construction of BFC and also enables us to avoid additional active component of the system, e.g., mediators, which sometimes are debated as interfering with different redox cycles in living cells. The project has shown that DET based BFC can be as powerful as mediated systems and by this encourages future innovative developments of environmentally friendly DET based devices. This is a very important and fundamental impact arising from the results of this project.

All scientists participating in this project were exposed to a broad spectrum of both fundamental and technological knowledge, and, equally important, they were trained in human resource management, gender- and ethics related problems, importance of public acceptance of advanced science/technology, and a business/IP-minded thinking. As the final result, in the second part of the project (month 18-36) a close dialogue with two companies, which are established in the relevant sectors (Energy and biotechnology sectors), was organised by Partner Mah with the support from MINC (www.minc.se) and Medeon (www.medeon.se) as described below.

The fundamental and technological knowledge developed during the project was discussed with CAVAC AB (www.cavac.se). Specifically, this young and ambitious Swedish company is interested in designing efficient and stable BFCs for different applications. Partner Mah was contacted by CAVAC as a possible party, which might provide technology to design efficient and stable cathodes. However, due to the lack of patents in this particular area (the Project was focused on biodevices instead of devices based on inorganic or organic catalysts) and financial constraints of the SME, no substantial agreement has been achieved so far.
Another example of commercialisation efforts from “3D-nanobiodevice” are in negotiations between the Finish company, VTT Biotechnology (www.vtt.fi) and Mah concerning a possible transfer of technology developed by researchers at Malmoe University during the project, specifically flexible, stable and efficient BFCs for extra vivo applications. Negotiations are ongoing and based on the patent WO/2011/117357 entitled: “Flexible biofuel cell, device and method” obtained by Mah with the financial support from “3D-nanobiodevice”.

Communication with the scientific community and the public at large was also an important task of "3D-nanobiodevice". Accumulation of knowledge and its faithful dissemination to the society fully supports the EC's policy on integrated, safe, and responsible nanotechnology. The Consortium hopes that these activities during the project were enable to increase both confidence and trust in the EC as a truly transparent and trustworthy communicator.

In addition to classical dissemination roots (publications in peer reviewed journals, conferences, workshops, symposiums, congresses, and public presentations) and novel/electronic means (web), results from the project were used in lectures, education programs, and other communication materials (newsletters, flyers, posters) via mass communication media. Detailed results on publications, patents, and disseminative activities of the Consortium are presented in the final report, as well as summarised in Table 6. It should be noted that generated foreground, which belong to industrial partners (NS and NZ) is mainly protected by know-how. It should be also emphasised that many additional publications and patents based on the foreground produced during the project, which are not mentioned in the dissemination activity list, will be published after the final report, e.g. a joint project patent (Mah, BOKU, and CSIC) concerning blood tolerant Lcs (D. Maté, D. Gonzáles-Pérez, M. Falk, R. Kittl, M. Pita, A.L. De Lacey, R. Ludwig, S. Shleev, and M. Alcalde "Human blood tolerant laccase" Tentative submission date: October, 2012), as well as a joint publication describing two final deliverables of "3D-nanobiodevce", viz. prototypes of self-contained biodevices for glucose and oxygen monitoring (3D-nanobiodevice consortium "Self-contained biodevices for glucose and oxygen monitoring" Tentative submission date: November, 2012). Moreover, the project webpage (www.mah.se/3Dnanobiodevice) will be functioning and updated at least for 5 years after the end of "3D-nanobiodevice". Furthermore, a short movie demonstrating scientific and technological achievements of the project including prototype tests will be designed and uploaded on the project webpage in the near future.

Table 1. Identity and composition (mole% added, and mol% determined by NMR where available) of the resulting polymer library

G160 DMAEMA(33%) BA(33%) St(26%) CbImPtn(8 %)
G294 AA(25%) BA(50%) EA(25%)
G316 MAA(33%) BA(55%) AGE-Im(11%l)
G399 AA(30%) BA(60%) PyImEA (10%) **NMR** : AA(23%) BA(70%) PyImEA (7%)
G400 AA(30%), BA(44%), St(18%),ImPyEA(8%)
G402 MAA(25%), BA(65%), ImPyEA(10%) **NMR:** MAA(27%), BA(64%), ImPyEA(8%)
G403 MAA(26%), BA(46%), St(19%), ImPyEA(8%)
G437 MAA(23%) BA(68%) ImEMA(14%)
G487 MAA 25% BA 75 %
G594 CbImEEMA 9%, BA 36%, DMAEMA 31%, St 23 %
G611 ImEMA 8%, BA 63%, AA 29%
G612 ImEMA 8%, BA 45%, AA 29%, EA 18 %
G613 ImEMA 8%, BA 27%, AA 29%, EA 36 %
G614 PyPMA 8%, BA 63%, AA 29%
G615 PyPMA 8%, BA 45%, AA 29%, EA 18 %
G616 PyPMA 8%, BA 27%, AA 29%, EA 36 %
G646 DMAEMA(34%) BA(60%) CbImEMA(7%)
G647 DMAEMA(30%) BA (20%) St(45%) CbImEEMA (5%)
G648 DMAEMA(34%) BA(20%) ThfA(40%) CbImEEMA(6%)
G702 AA (31%) BA(44%) 6f-BA(25%)
G703 AA (30%) BA (43%) AcacEA (28%)
G704 AA (31%) BA(45%) CHMA(24%)
G705 MAA(26%) BA(47%) 6f-BA(26%)
G706 MAA(25%) BA (45%)AcacEA(29%)
G707 MAA(27%) BA (48%) CHMA (26%)
G737 ImPyEEMA 7%, BA 27%, AA 10%, St 17 %, LMA 13%, EHA 19%, AllMA 5%
G738 ImPyEEMA 7%, BA 38%, AA 10%, St 16 % , LMA 6%, EHA 18%, AllMA 5%
G779 PyImEEMA (7%) BA (63%) MAA (31%) **NMR**: PyImEEMA (6,6%) BA (62,9%) MAA (30,6%)

Table 2. List of selected polypyridyl-based redox complexes, and the redox potentials for $Os^{2+/3+}$ transition in acetonitrile solvent.

dmbim is dimethylbiimidazole, dabpy is diaminobipyridine, dmobpy is dimethoxybipyridine, dmbpy is dimethylbipyridine, bpy is bipyridine, phen is phenanthroline, dclbpy is dichlorobipyridine, L3 is isonicotinic acid, L4 is 4-aminomethylpyridine and L6 is 4-aminoethylpyridine.

Complex	*$E^{o\prime}$ (V vs. Ag/AgCl)*
$Os(dmbim)_2Cl_2$	-0.69
$Os(dabpy)_2Cl_2$	-0.66
$Os(dmobpy)_2Cl_2$	-0.27
$Os(dmbpy)_2Cl_2$	-0.12
$Os(bpy)_2Cl_2$	0
$Os(phen)_2Cl_2$	0.01
$Os(dclbpy)_2Cl_2$	0.2
$[Os(bpy)_2Cl(L3)].\ PF_6$	0.25
$[Os(bpy)_2Cl(L4)].\ PF_6$	0.27
$[Os(bpy)_2Cl(L6)].\ PF_6$	0.26
$[Os(dcbpy)_2Cl(L3)].\ PF_6$	0.41
$[Os(dcbpy)_2Cl(L4)].\ PF_6$	0.44
$[Os(dmbpy)_2Cl(L3)].\ PF_6$	0.11
$[Os(dmbpy)_2Cl(L4)].\ PF_6$	0.15
$[Os(dmbpy)_2Cl(L6)].\ PF_6$	0.18
$[Os(dmobpy)_2Cl(L4)].\ PF_6$	0.09
$[Os(dmobpy)_2Cl(L6)].\ PF_6$	0.03

Table 3. List of selected redox polymers, and associated redox potentials, prepared by reaction of Os complexes from Table 2 with poly-N-vinylimidazole (PVI), as shown in the scheme below.

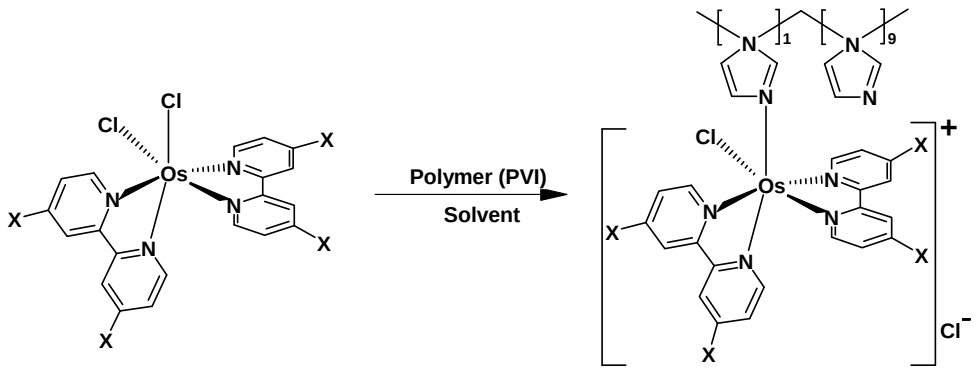

Polymer I:	$[Os(bpy)_2(PVI)_{10}Cl]^+$	$E^0 = 228$ mV
Polymer II:	$[Os(dclbpy)_2(PVI)_{10}Cl]^+$	$E^0 = 304$ mV
Polymer III:	$[Os(dmbpy)_2(PVI)_{10}Cl]^+$	$E^0 = 124$ mV
Polymer IV:	$[Os(phen)_2(PVI)_{10}Cl]^+$	$E^0 = 240$ mV
Polymer V:	$[Os(dmobpy)_2(PVI)_{10}Cl]^+$	$E^\circ = -43$ mV

Table 4. Identity of selected redox polymers, and associated redox potentials, prepared by reaction of $Os(bpy)_2Cl_2$ with the selected polymer from Table 1, as shown in the scheme.

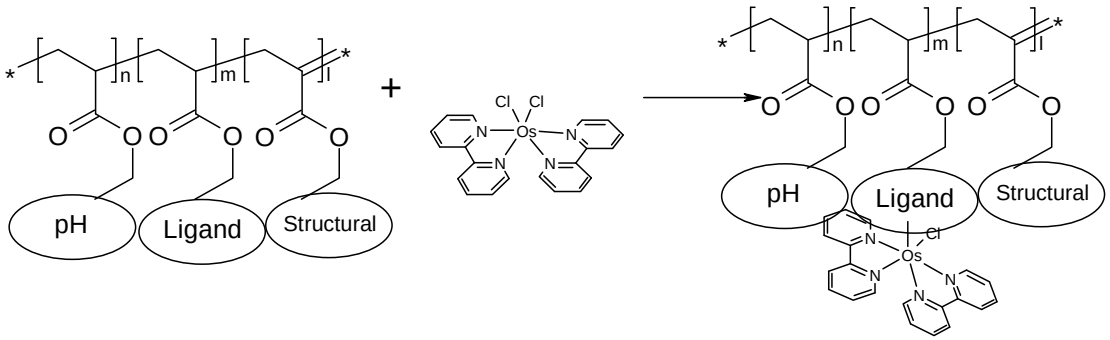

G235: based on G160 OsBiPy(28%) LS, DPV: -20 mV (main); +230 mV vs Ag/AgCl
G405: based on G399 OsBiPy(1.5%) LS, DPV: ca.+514 mV(main); +308 mV vs SCE
G428: based on G316 OsBiPy(5.7%) DPV:+60 mV vs SCE
G440: based on G437 OsBiPy(16%) DPV:+80 mV vs SCE;
G490: based on G487 $Os(Bipy)_2$ ca. 2 % DPV: -182 mV(main), 240 mV vs Ag/AgCl
G504: based on G294 Os(BiPy)2 ca. 20% DPV: ca.-160 mV, +220 mV s Ag/AgCl
G604: based on G594 $Os(BiPy)_2$ ca. 4.5 % DPV: -20 mV (main), 250 mV vs Ag/AgCl
G617: based on G611 $Os(Bipy)_2$ ca. 3 % DPV: +104 mV vs Ag/AgCl
G618: based on G612 $Os(BiPy)_2$ ca. 3 % DPV: +120 mV vs Ag/AgCl
G619: based on G613 $Os(BiPy)_2$ ca. 3 % DPV: 116 mV vs Ag/AgCl
G620: based on G614 $Os(BiPy)_2$ ca. 3 % DPV: +278 mV vs Ag/AgCl
G621: based on G615 $Os(BiPy)_2$ ca. 3 % DPV:+302 mV vs Ag/AgCl
G622: based on G616 $Os(BiPy)_2$ ca. 3 % LS, DPV: +275 mV vs Ag/AgCl
G649: based on G646 OsBiPy(4.5%) LS, DPV: ca.-4 mV(main); +280 mV vs Ag/AgCl
G650: based on G647 OsBiPy(4.6%) LS, DPV: : ca.-14 mV(main); +257 mV vs Ag/AgCl
G651: based on G648 OsBiPy(4.6%) LS, DPV: : ca.-12 mV(main); +263 mV vs Ag/AgCl
G697: based on G400 OsBiPy(1.4%) LS, DPV: ca.+480 mV(main); +300 mV vs Ag/AgCl
G698: based on G402 OsBiPy(1.5%) LS, DPV: ca.+490 mV; +270 mV(main) vs Ag/AgCl
G699: based on G403 OsBiPy(1.6%) LS, DPV: ca.+490 mV(main); +270 mV vs Ag/AgCl
G708: based on G702 Os(bipy)2 ca. 6.9% DPV: -190 mV(main), +246 mV, +420 mV vs SCE
G709: based on G703 Os(bipy)2 ca. 7.1% DPV: -160 mV vs SCE
G710: based on G704 Os(bipy)2 ca. 7.0% DPV: -180 mV, +250 mV,+ 416 mV (main)
G711: based on G705 Os(bipy)2 ca. 7.1% DPV: -190 mV(main), +250 mV, +440 mV vs SCE
G712: based on G706 Os(bipy)2 ca. 7.2% DPV: -200 mV vs SCE
G713: based on G707 Os(bipy)2 ca. 7.2% DPV: -220 mV (main), +227 mV vs SCE
G746: based on G737 OsBiPy(1.7%) DPV: +425 mV vs SCE
G747: based on G738 OsBiPy(1.8%) DPV: 155 mV , +430 mV(main) vs SCE
G814: based on G779 OsBiPy(4.5%) LS, DPV: ca.+500 mV vs SCE
G819: based on G779 OsBiPy(1.4%) LS, DPV: ca.+520 mV vs SCE

Table 5. Estimative economic feasibility of designed biodevices		
Devices	in 3 years (M€)	in 10 years (M€)
Potentially implantable microbiosensor towards glucose	20	50
Potentially implantable microscale wireless self-powered biodevices for continuous glucose monitoring	0	120

Table 6. Dissemination of foreground					
Beneficiary	Scientific papers, Review, Book chapters, and Books	Patents	Theses (Master and PhD works)	Conferences, Workshops, Symposiums, Congresses, and Meetings	Other disseminative activities (flyers, articles, press releases, presentations at schools and colloquiums, other publications)
P1. Mah	10	1	0	3	6
P2. NS	0	0	0	0	0
P3. AU	1	0	0	2	0
P4. RUB	5	0	0	11	0
P5. UL	2	0	0	9	0
P6. BOKU	6	1	7	16	1
P7. CSIC	10	2	2	12	8
P8. ULUND	11	2	1	32	0
P9. NUIG	2	0	0	11	1
P10. US	1	0	0	7	0
P11. NZ	0	0	1	0	0
In Total:	48	6	11	105	16

Figure 1. *(A) Principal scheme of a self-contained bioelectronic device for biomedical applications.*
(B) *Self-contained biodevice for glucose monitoring in human physiological fluids.*

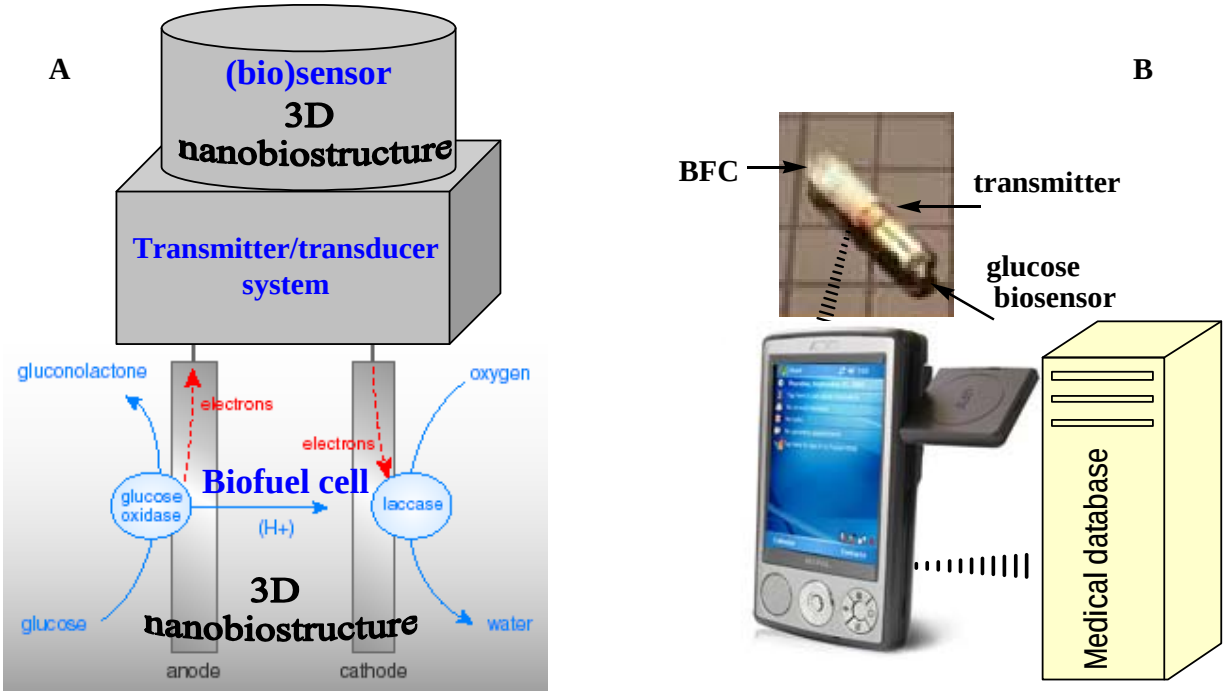

Figure 2. *Pictures from the final test of self-contained biodevices.*
*(**A**) Picture of an oxygen sensitive wireless self-powered biodevice, i.e. a biofuel cell (glass cell with electrodes and cables marked with a red arrow) connected to the wireless operational unit (white box) and a control device (yellow voltmeter).*
*(**B**) Personal computer with a wireless receiver (marked with a red arrow).*

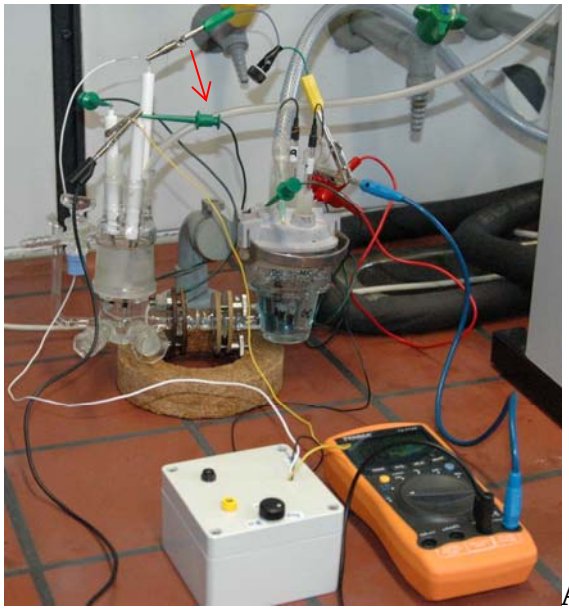

A

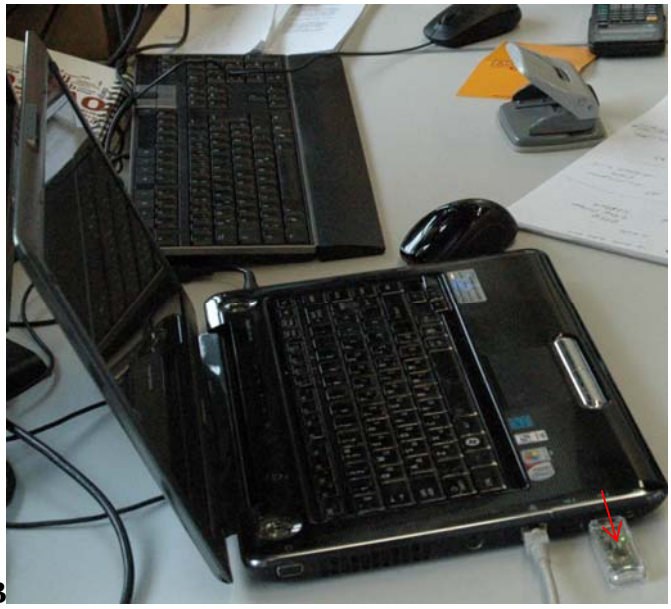

B

Figure 3. *Location of "3D-nanobiodevice" project in modern technology network.*

(from S.S. Mehta's book "Commercializing successful biomedical technologies" with some modifications and additions)

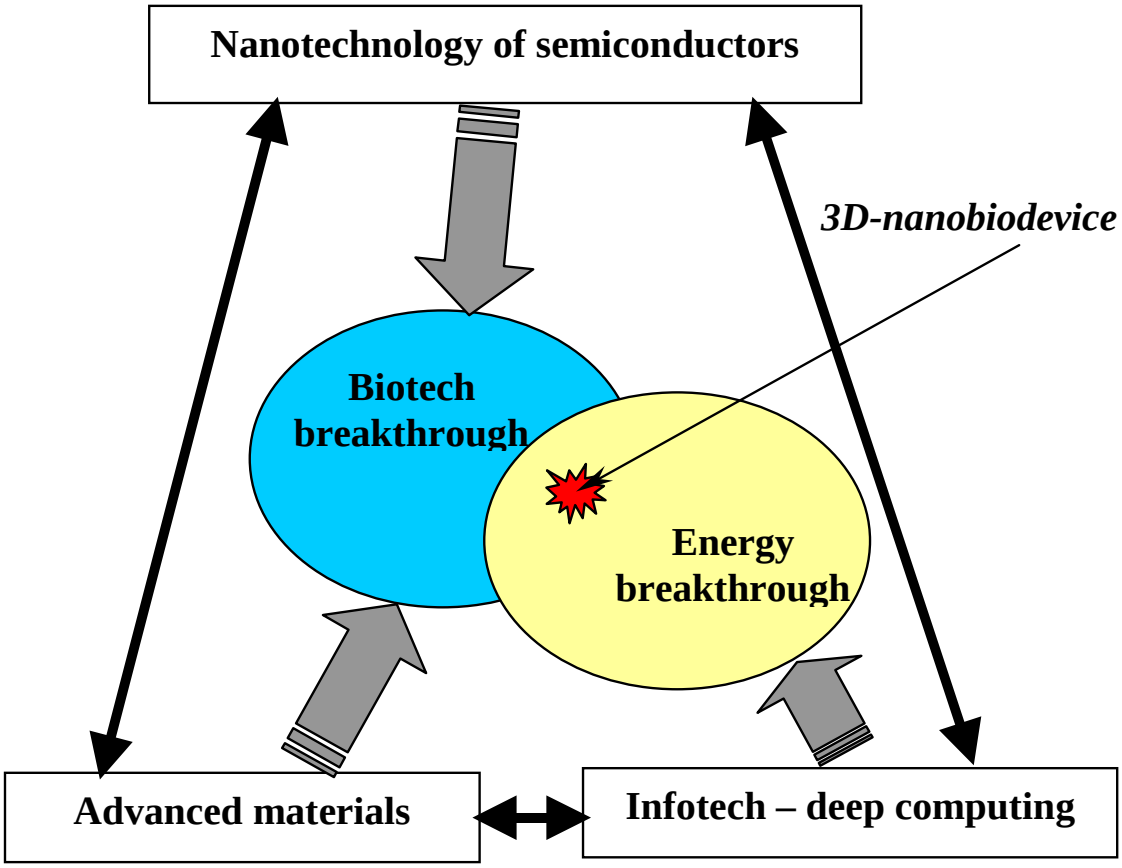

Figure 4. *Developed transmitter/receiver system*

Radio prototype with folded 2.45GHz antenna

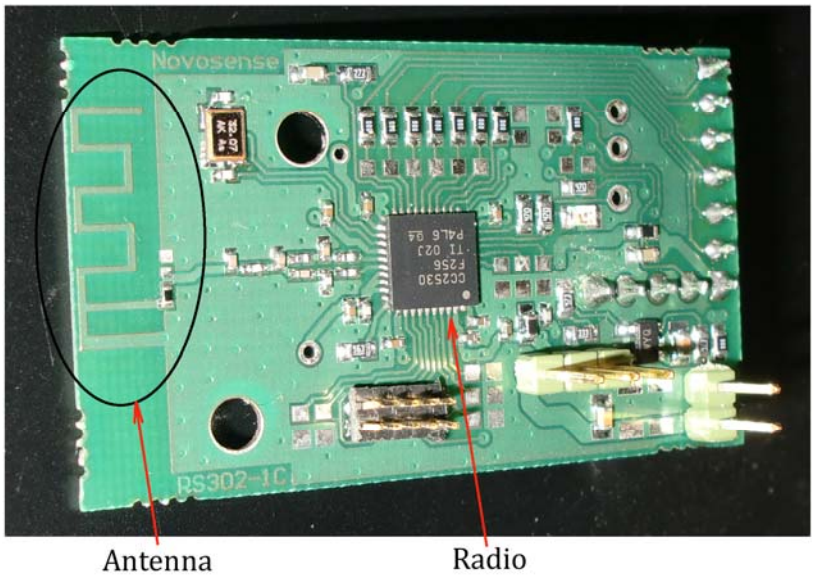

Receiver with USB connector for easy connection to a PC

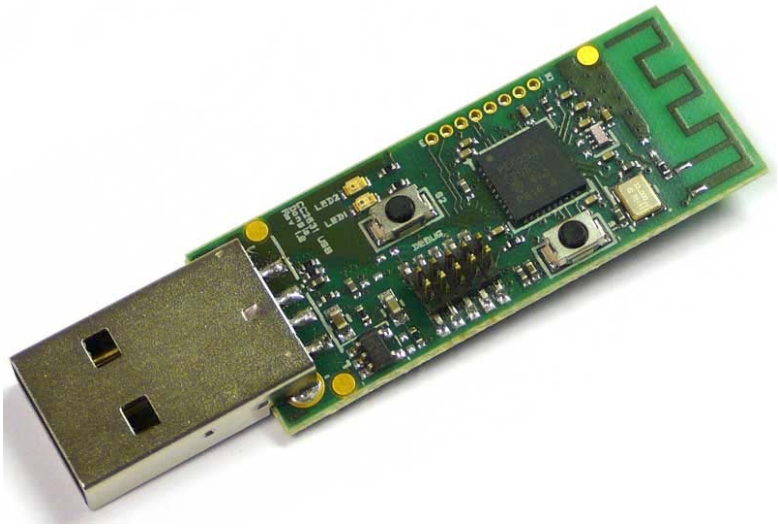

Figure 5. *3D nanostructure fabricated and characterised by the Consortium*

HMPSi

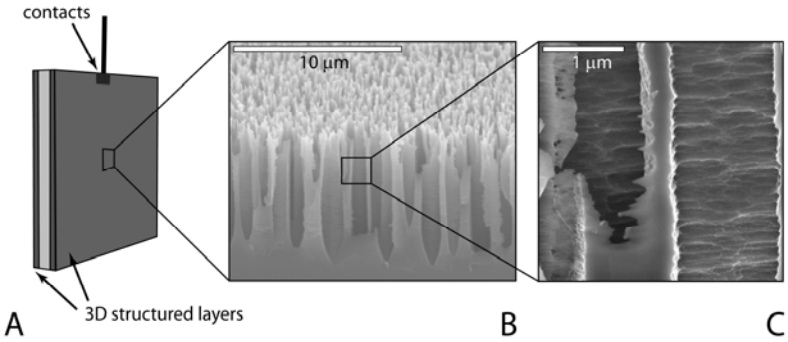

HTGCNT

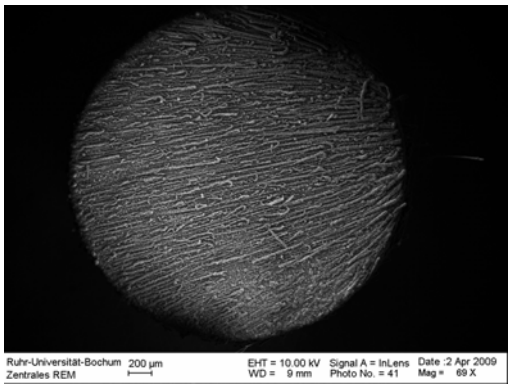

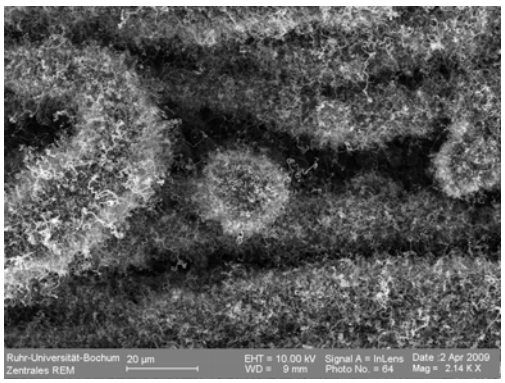

OAN

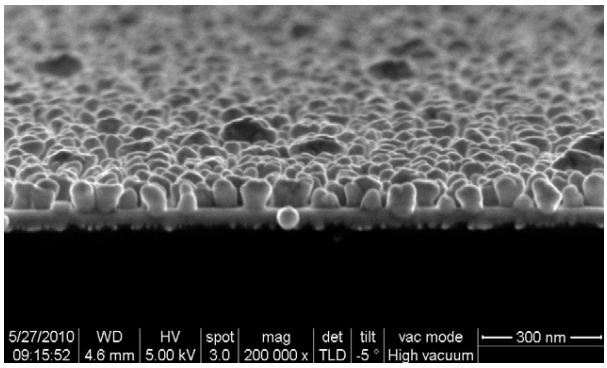

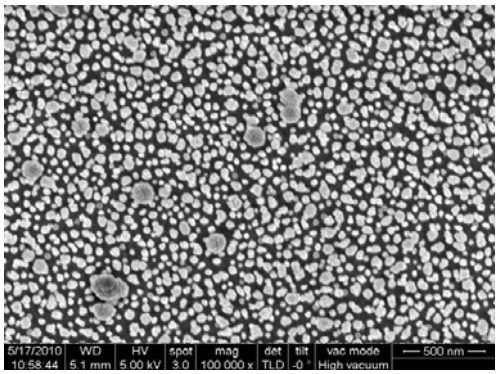

CMP

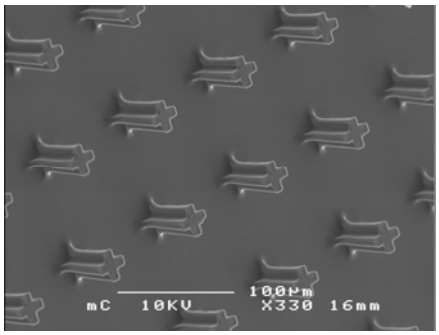

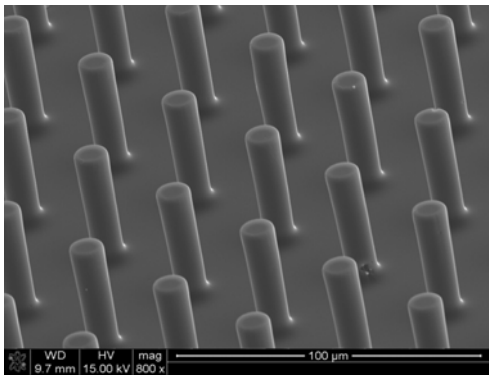

Figure 6. *Produced bioelements*

Glucose oxidising redox enzyme

Cellobiose dehydrogenase

Glucose oxidase

Oxygen reducing redox enzyme

Laccase

Bilirubin oxidase

Figure 7. *Library of Os and Ru containing redox polymers*

Figure 8. *Fabricated biochips based on three-dimensional nanostructures*

NMPSi

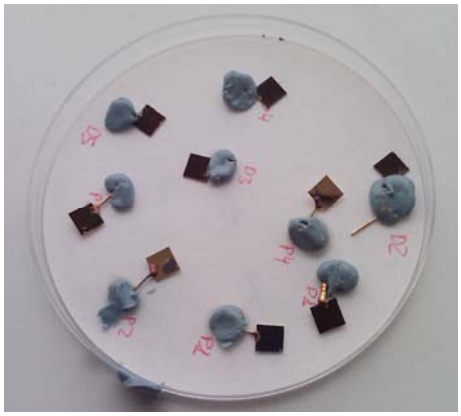

NMPSiT

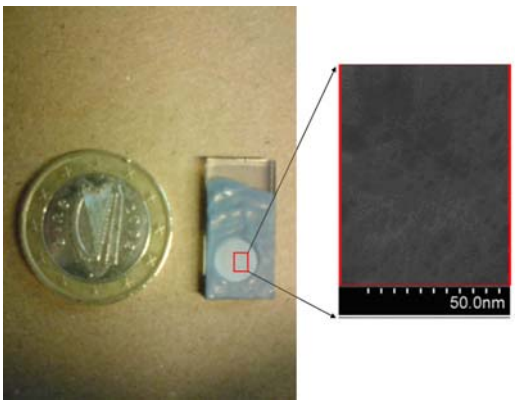

OAN

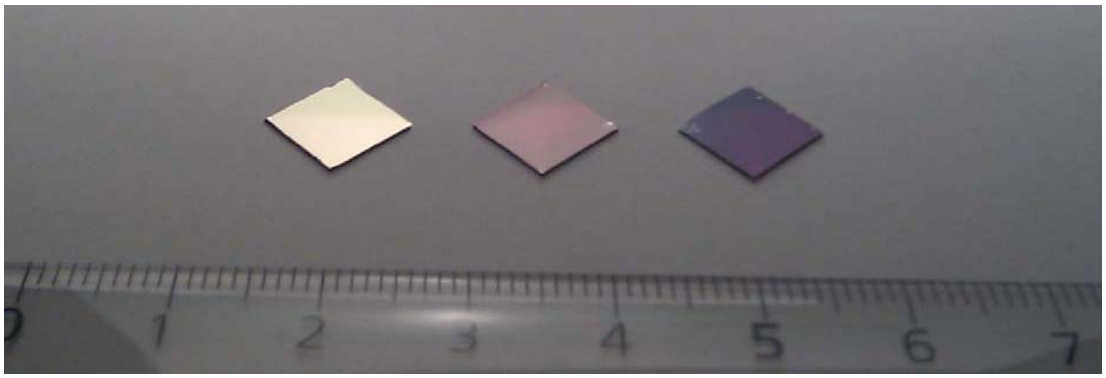

HTGCNT

CMP array

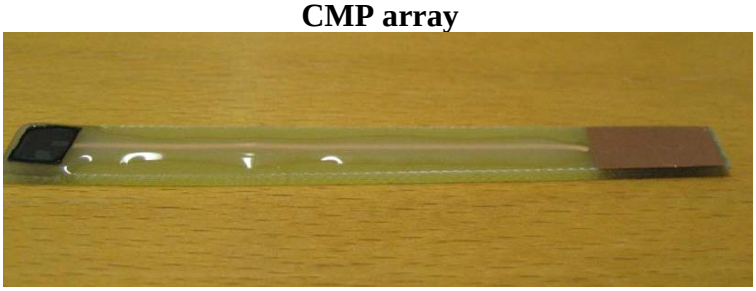

Figure 9. 1*) Setting-up procedures for biomedical experiments*

Collection of physiological liquids
(blood, plasma, serum, saliva) including final preparation of protocols, selection of donors , etc.

Arrangement of methods for biomedical characterisation of physiological liquids*:*

- *determination of glucose (HemoCue Glucose 201⁺Analyzer)*

- *total protein content (Bio-Rad Assay)*

- *oxygen concentrations (OxyGraph)*

2*) Collection of human physiological fluids*
A – blood, serum, plasma; B – saliva

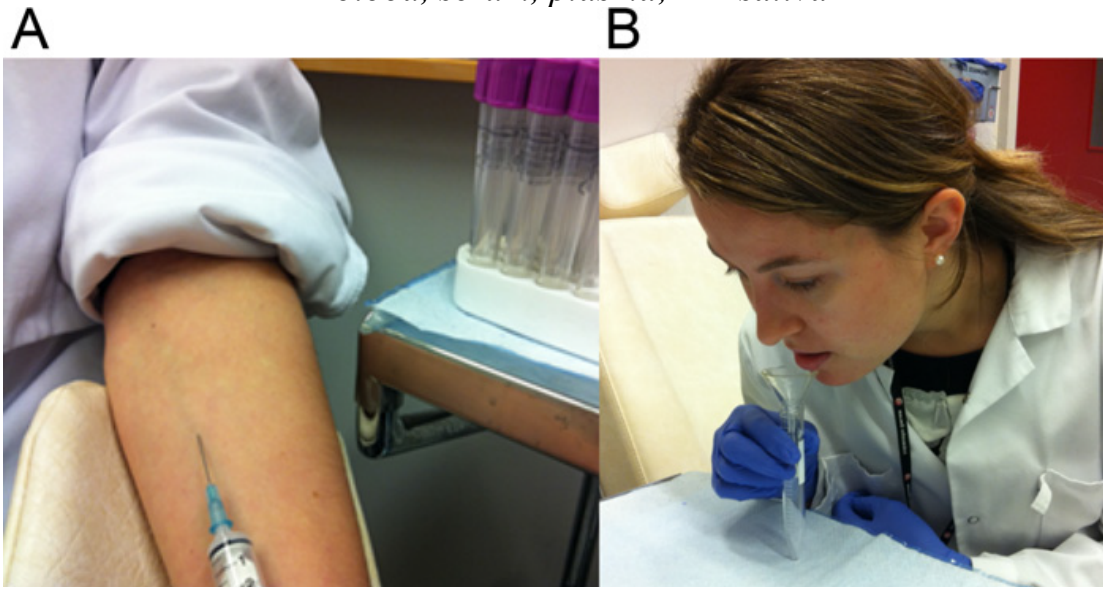

Figure 10. *Characterisation of 3D biodevices in human physiological fluids*

Using macroscale (total volume 10 mL) electrochemical cell
(studies in blood, serum, and plasma)

Using microscale (total volume 10 μL) electrochemical cell
(studies in saliva)

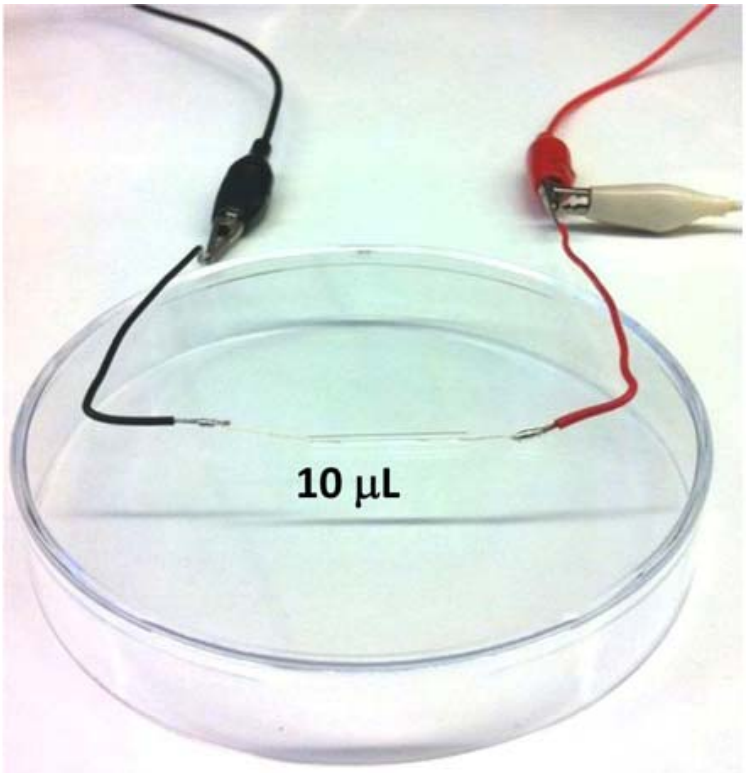

Figure 11. 1*) Cell culture plates with disposable electrode arrays*

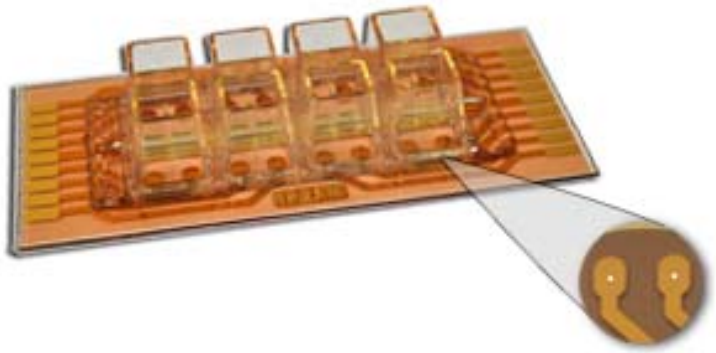

2*) Cell culturing on different surfaces including biomodified nanostructured electrodes*

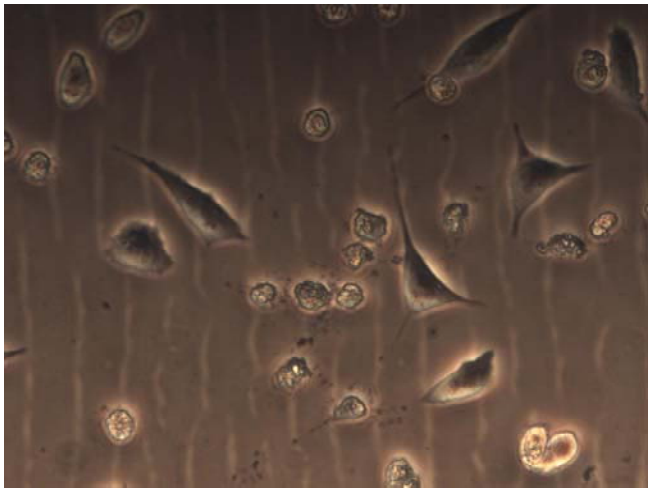

L929 cells incubated at PEI-modified surface.

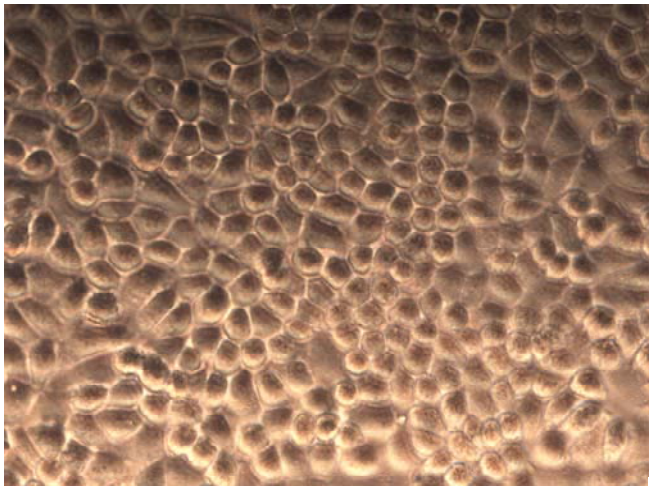

L929 cells incubated at PEI/SWCNT/CHI-modified surface.

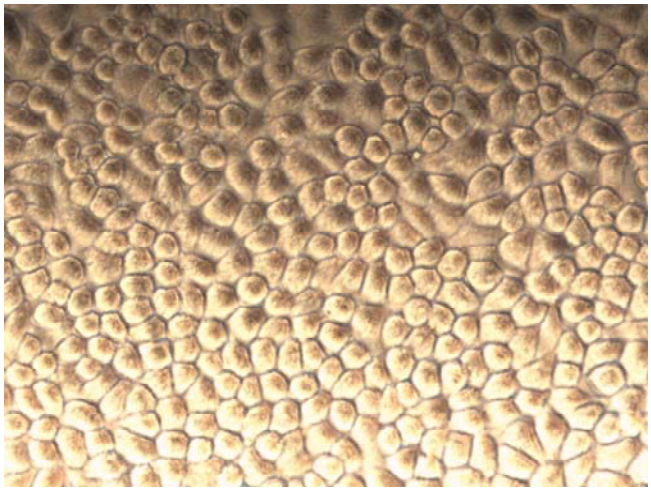

Control cells incubated in culture medium.

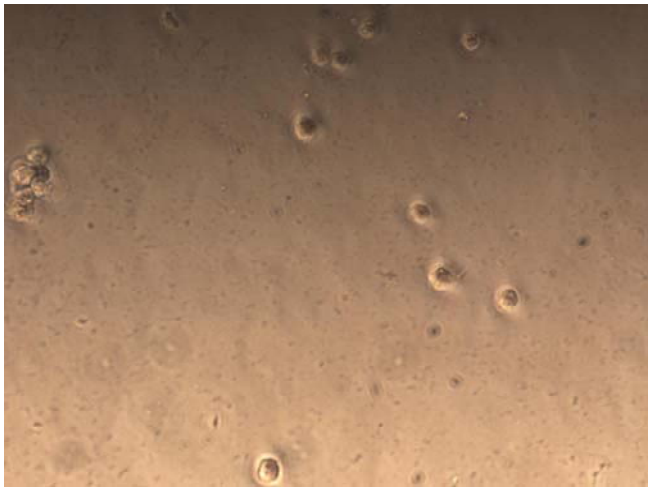

L929 cells incubated at PEI/SWCNT/CHI/GOx-modified surface.

Figure 11. *Schematic illustration of the procedure used to prepare carbon post microarrays.*

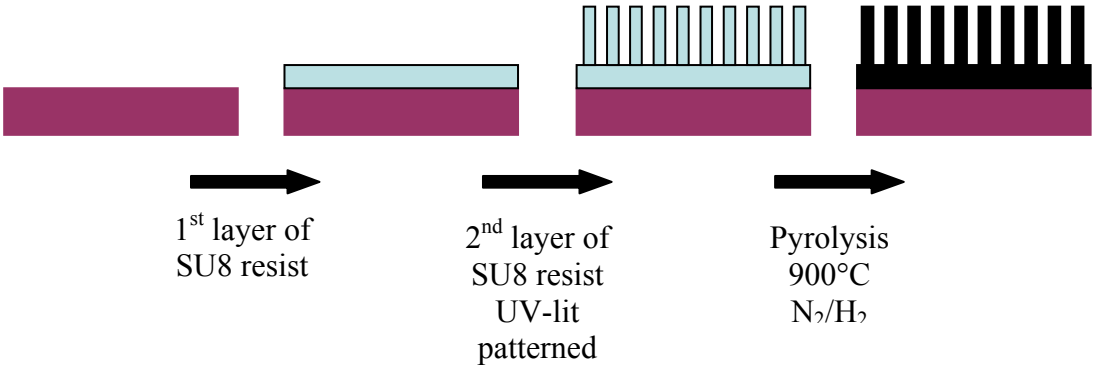

Figure 12. *SEM image of SU8 posts on silicon before pyrolysis.*

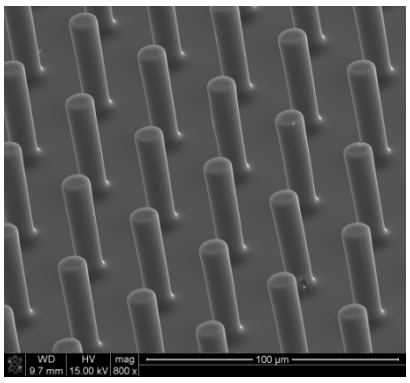

Figure 13. *Graphite CPM mounted on PCB.*

Figure 14. *Three-dimensional structured silicon chips. (A) Schematic illustration of the NMPSi chip. Both sides of the electrode are covered with micro-/ nanostructured silicon layers. (B) Scanning electron micrograph of the 3D layer. The layer depth is 10 μm. (C) Zoom into a typical surface (left column, top view; right column, side view). The macropores of micrometer size are clearly seen, combined with nano-morphology (50–300 nm).*

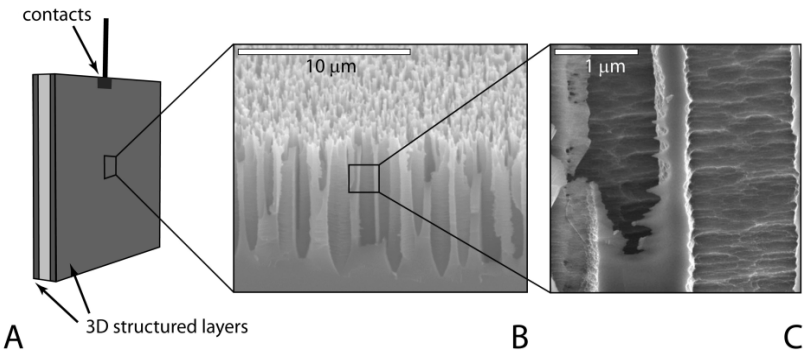

Figure 15. *Picture of (A) an FTO electrode chip with inset showing an SEM image of the silicate pores and (B) a nanoporous gold electrode.*

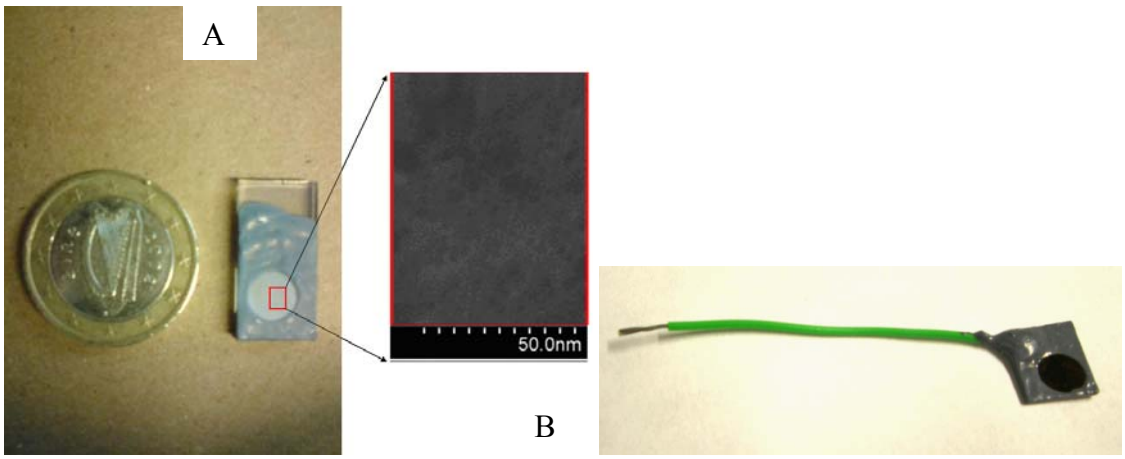

Figure 16. *SEM images of (A) a graphite rod modified with carbon microfibres, (B) carbon microfibers under high magnification, (C) CNT modified carbon microfibres at low magnification and*
(D) – (F) CNT modified carbon microfibres at high magnification.

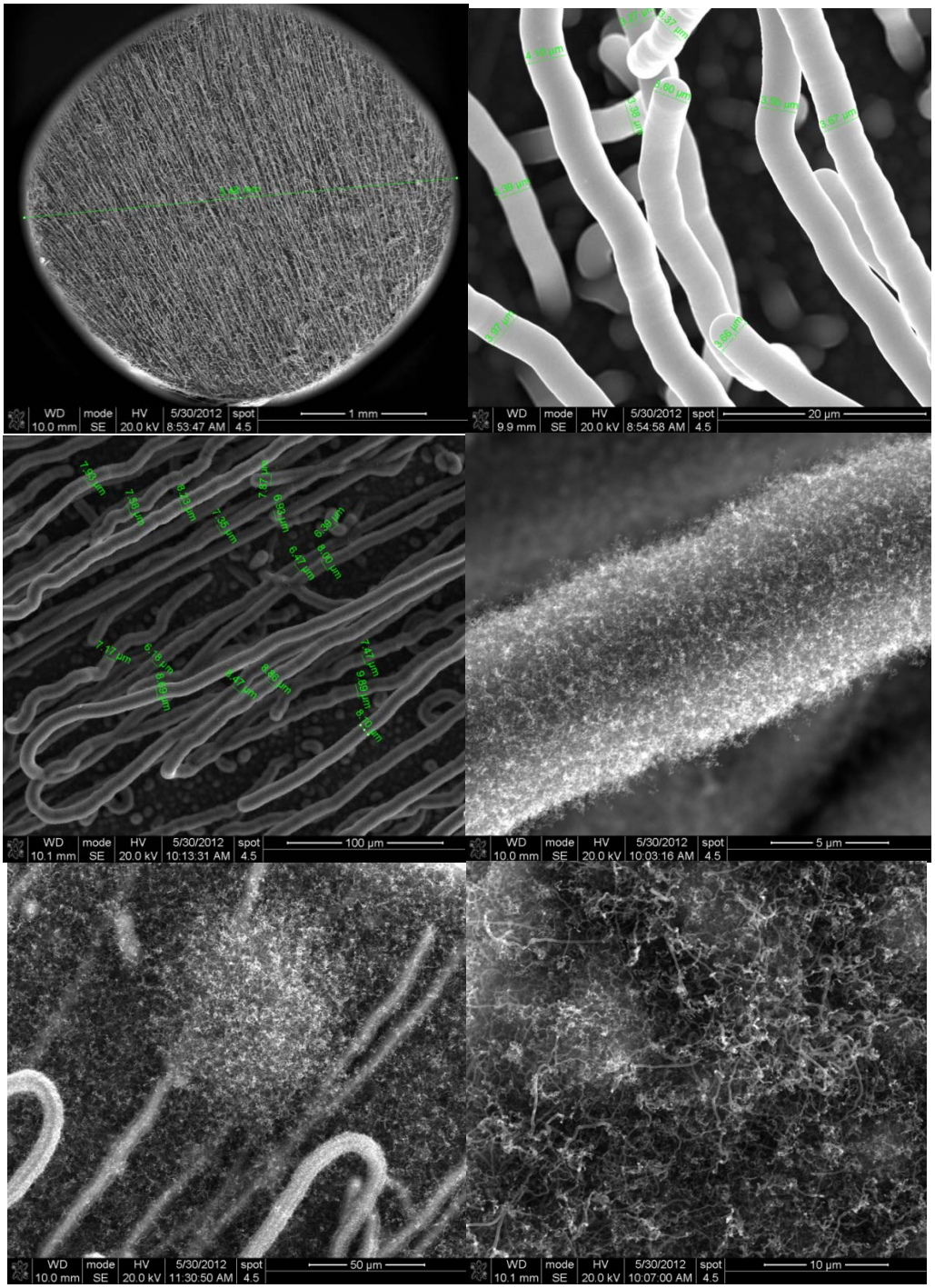

Figure 17. *SEM images of ordered assemblies of nanostructures.*

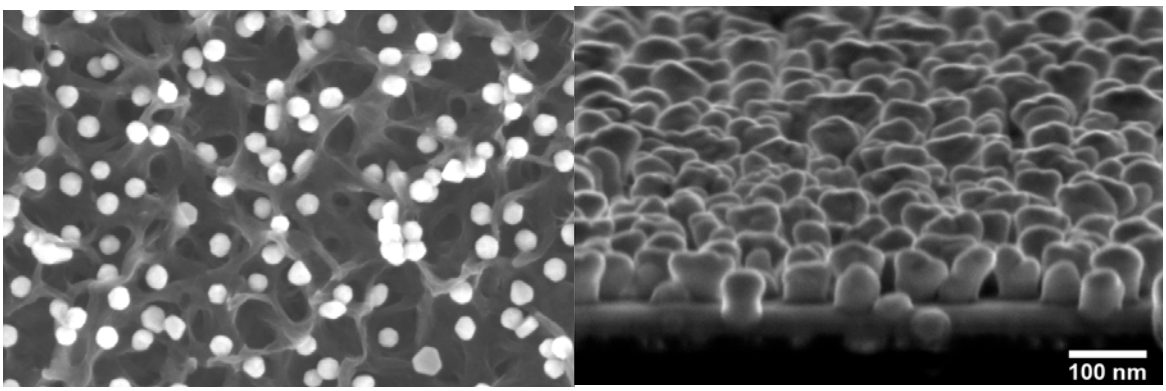

Figure 18. *Representative example of fungal cultures for oxidoreductase screening.*

Figure 19. *Electron transfer pathway and kinetic analysis of electron transfer rates in cellobiose dehydrogenase. Left: Schematic presentation of the catalytic reaction (CAT, yellow) which ocurrs in the flavodehydrogenase domain (blue). This step is followed by the intramolecular electron transfer (IET, red) which shuttles an electron to the cytochtome domain (red) and further to the electrode (grey) by the direct electron transfer step (DET). Right: Fast kinetic analysis by stopped-flow photometry was used to elucidate the rate constants of the electron transfer steps. The shown multiple variant of M. thermophilum CDH has an increased IET (grey line) following the catalytic turnover at the FAD (black line). The inset uses a logarithmic time scale.*

A

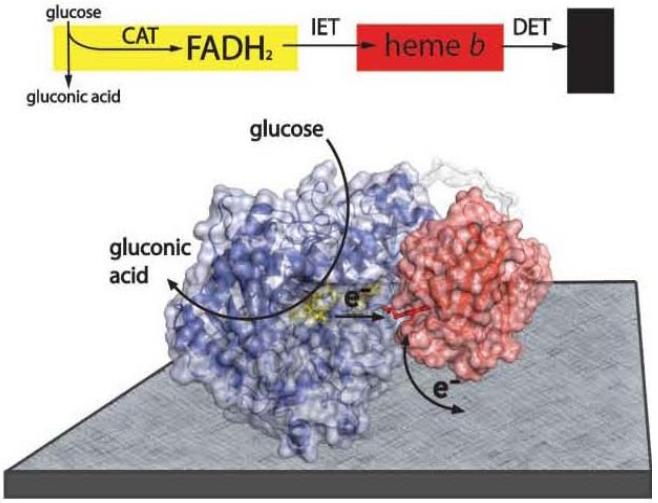

B

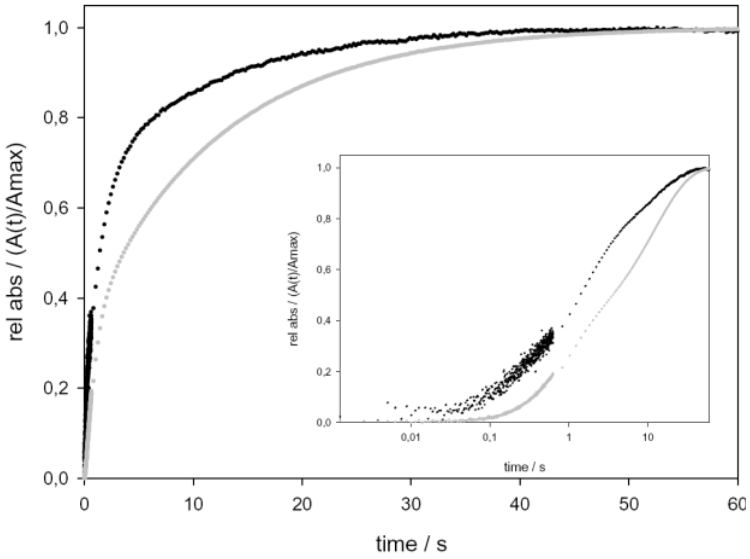

Figure 20. *Docking studies on a generated model of HiCDH FAD-domain. A model of ß-D(+)-Glucose was docked into the putative active site of HiCDH FAD-domain, and the resulting model used to map potential interactions for active-site redesign.*

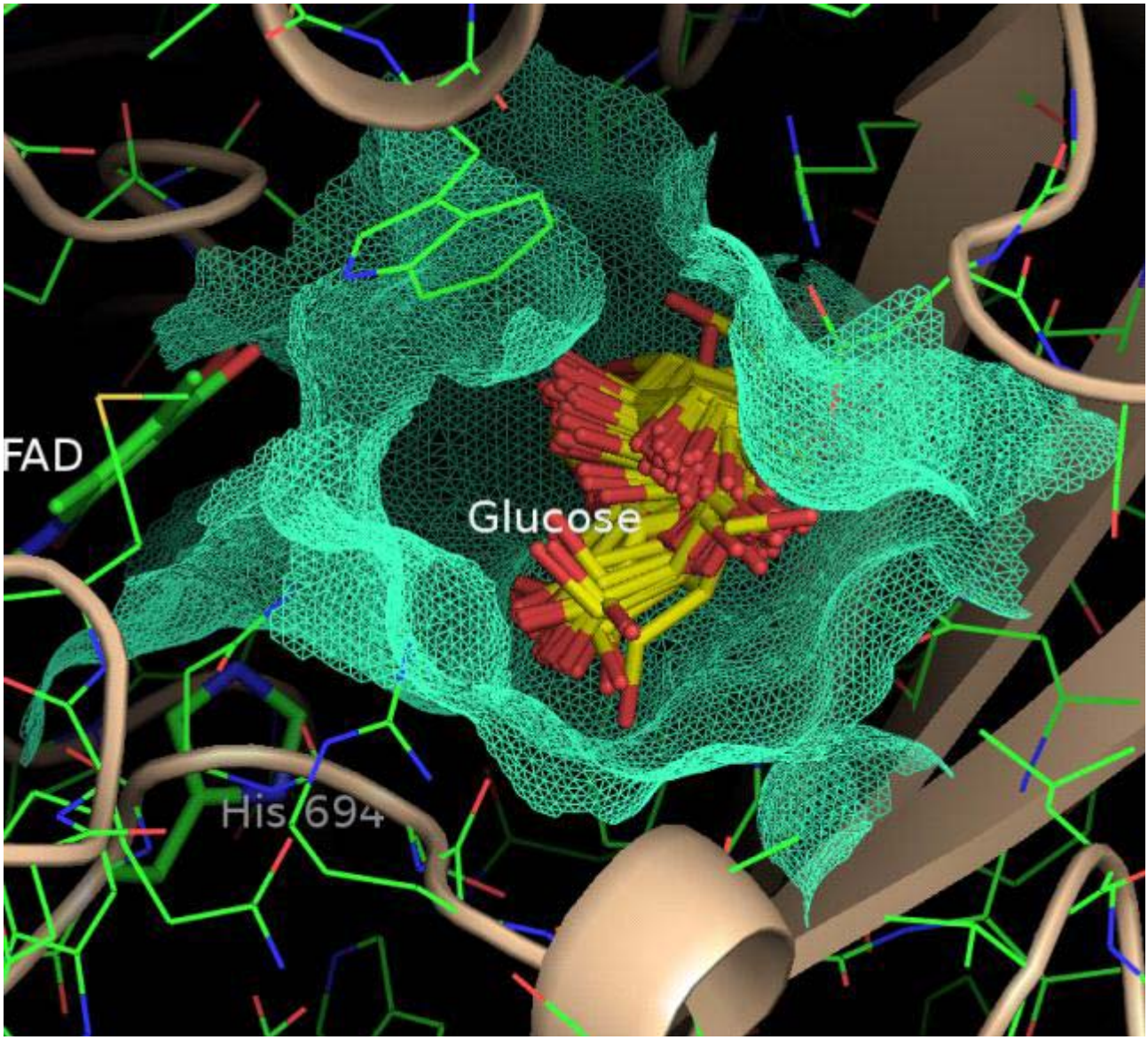

Figure 21. *Screening assays to measure carbohydrate dehydrogenase activity of CDH.*
Left - the reduction of dichlorophenolindophenol (DCPIP), observed by a decrease in absorbance at 520nm and the bleaching of DCPIP's blue color, occurs directly at the FAD active site and can be used to determine enzyme expression (it's also a good measure of enzyme potential for MET).
Right - reduction of cytochrome c, observed by an increase in absorbance at 550nm and a change in color from orange (oxidized) to pink (reduced), occurs only at the HEME domain and therefore requires interdomain electron transfer (it can be used to measure enzyme potential for DET).

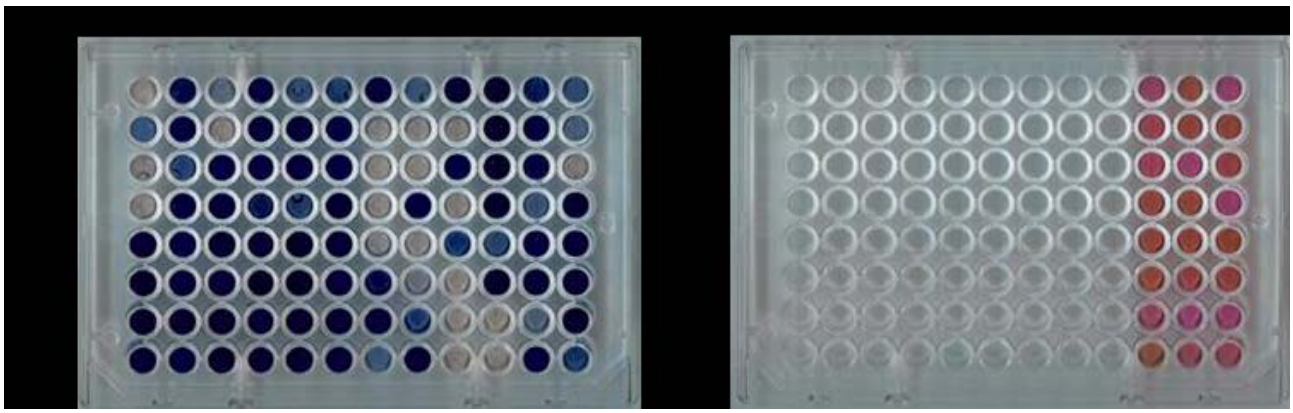

Figure 22. *Schematic representation of the cathodic reaction (reduction of O_2) catalyzed by immobilised laccase or bilirubin oxidase. The mechanism involves direct electron transfer from the electrode (grey) to the T1 copper center in the enzyme, followed by intramolecular electron transfer to the T2/T3 copper site, where the reduction of O2 takes plate, generating water as the final product.*

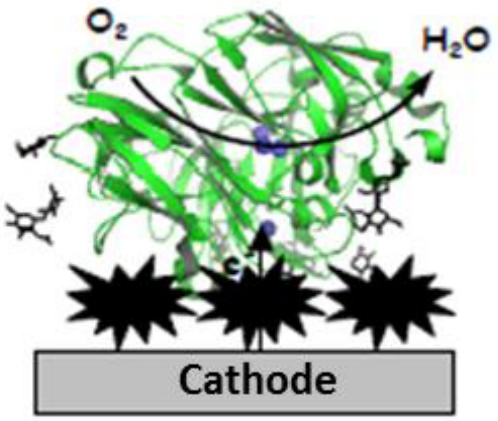

Figure 23. *Schematic view of the strategy used for directed evolution of thermostable PM1 laccase variants, from diversity generation to colony picking and screening.*

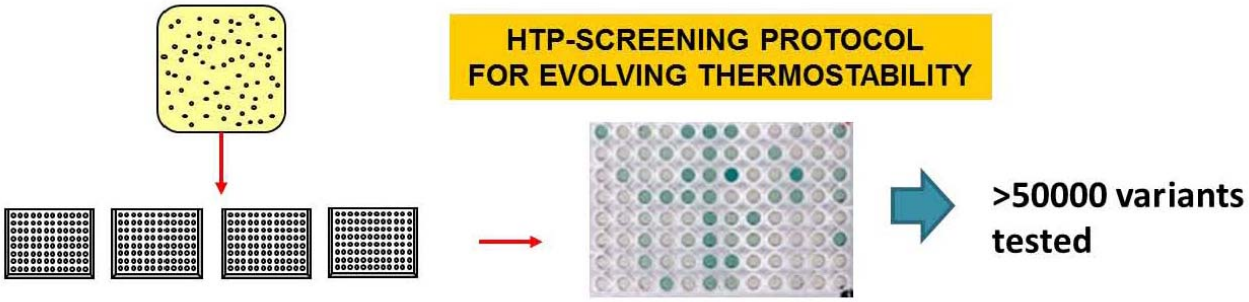

Figure 24. *Structures and abbreviations for the range of monomeric components used in combinations for production of the library of polymers.*

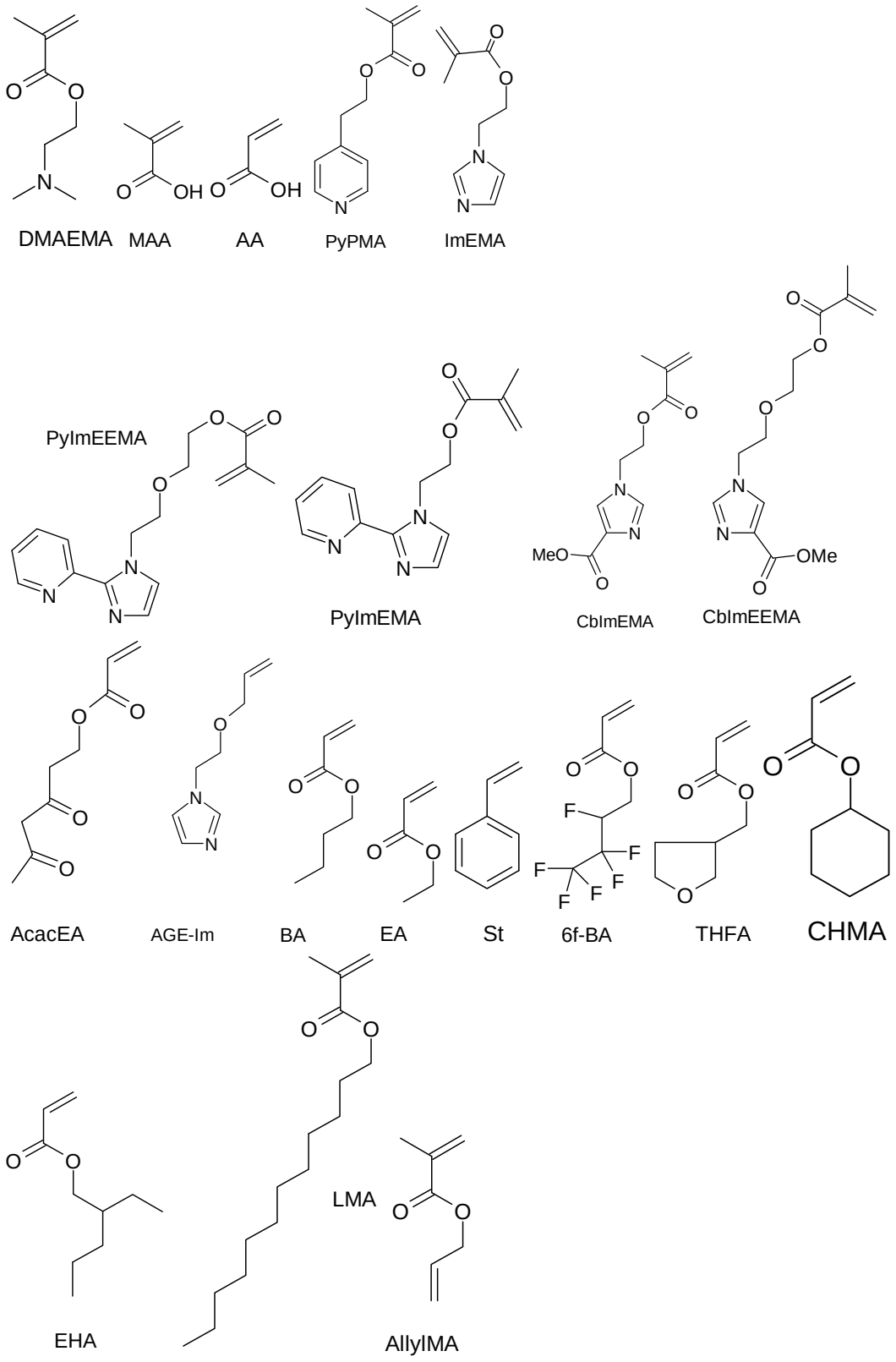

Figure 25. *The effect of polymer composition on the range of oxygen reduction current densities as a function of enzyme loading within a redox polymer/laccase film on carbon electrodes.*

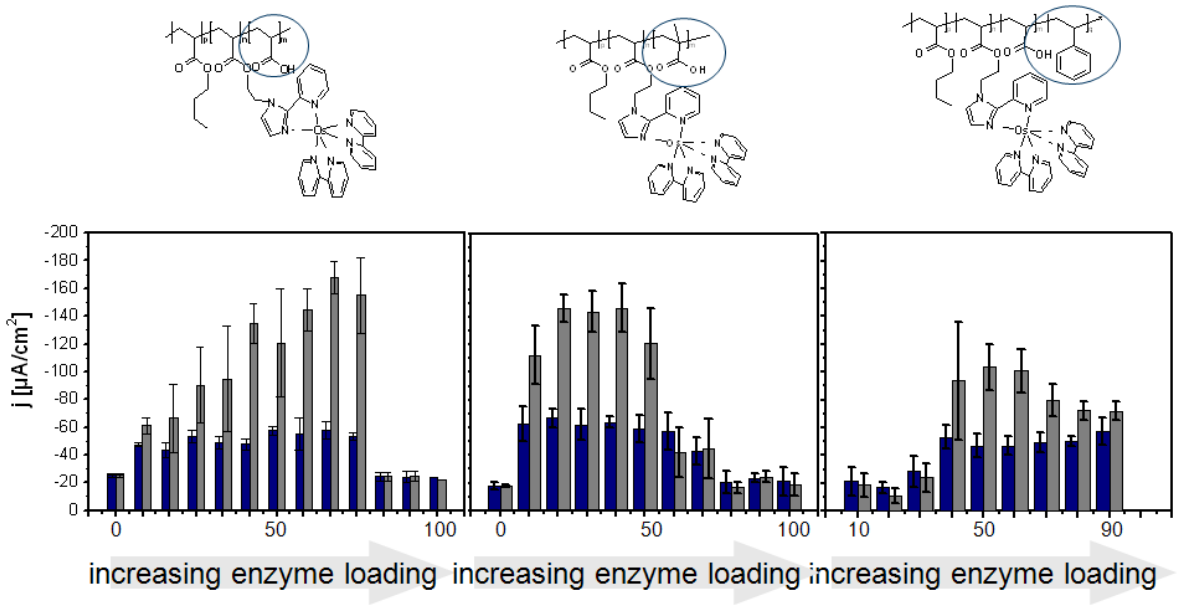

Figure 26. *Effect of ratio of glucose oxidase (GOx) to redox polymer (Polymer I) (left), and of the addition of CNT and crosslinking approach (GA is glutaraldehyde and PEG is polyethyleneglycol diglycidyl ether) on glucose oxidation current.*

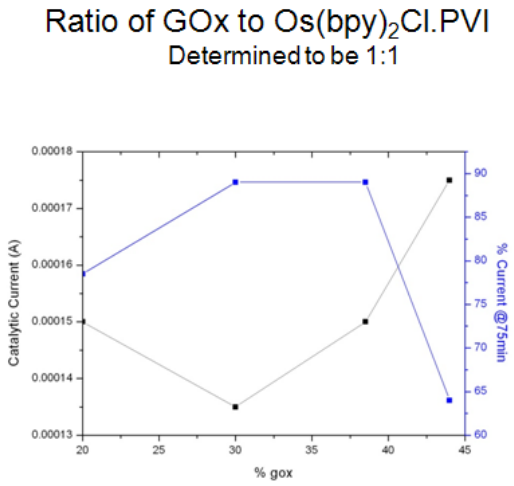

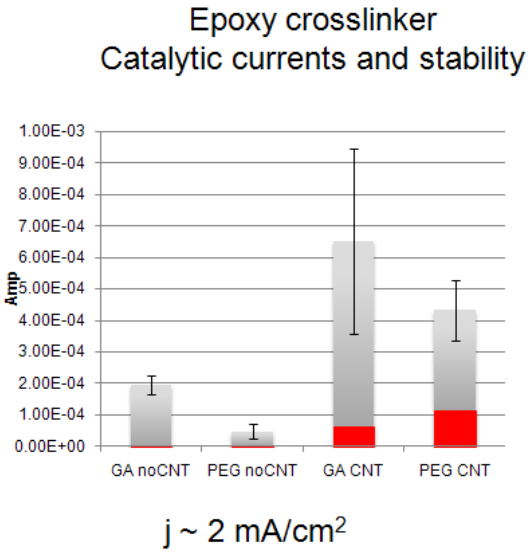

Figure 27. *Cyclic voltammetry of glucose oxidase / redox polymer I at a nanoporous gold electrode in the presence of increasing concentration of β-D-glucose.*

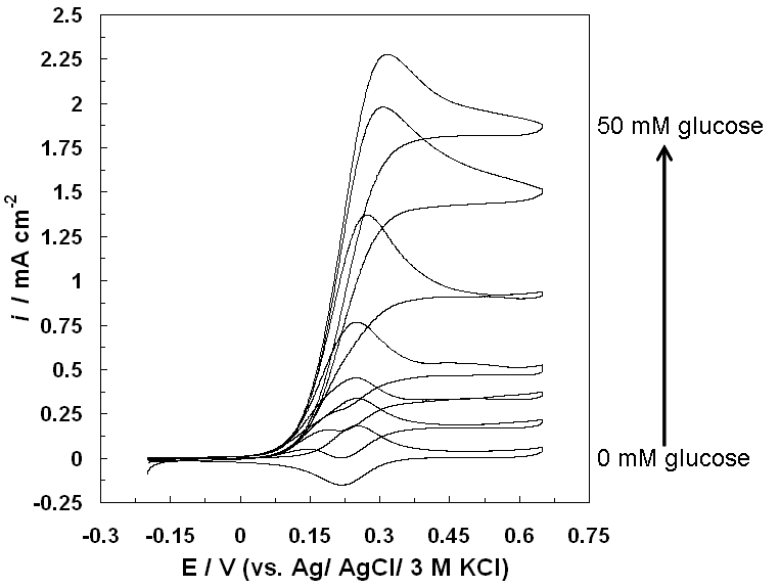

Figure 28. *SEM images of the 3D-microarray electrode.*

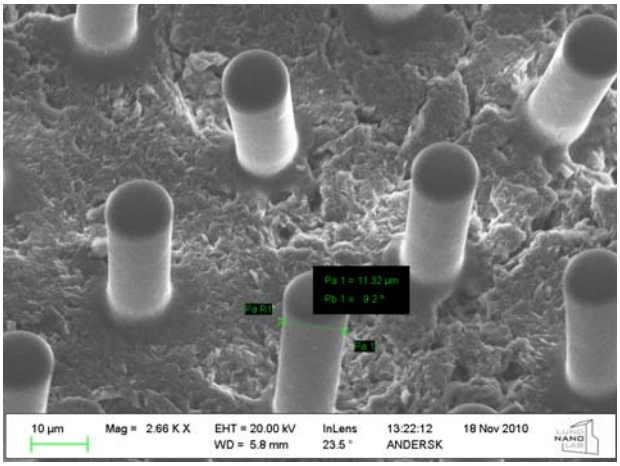

Figure 29. *LSV of CtCDH/SWCNT/3D-micropost (a) in pH 7.4, 50 mM phosphate buffer containing 5 mM lactose (black line); (b) in pH 7.4, 50 mM phosphate buffer containing 5 mM glucose (red line). Scan rate: 1 mV·s^{-1}. RE: Ag/AgCl$_{sat}$.*

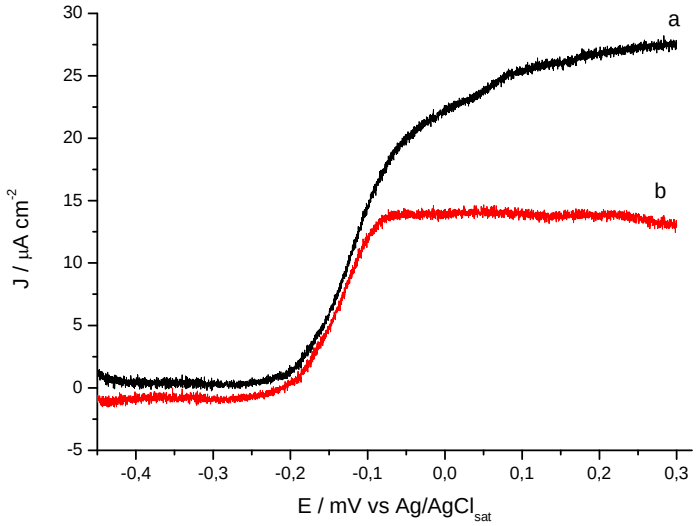

Figure 30. *Biocatalytic current recorded at CMF/CNT graphite electrode modified with TvCDH, in absence (black line) and in presence of 10 mM lactose (red line).*

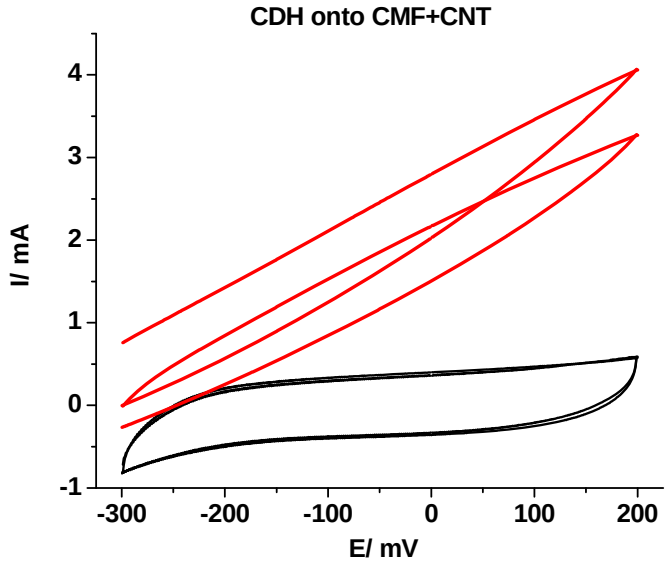

Figure 31. *(A) SEM pictures of 3D-CMF/CNT electrodes. (B) Biocatalytic current recorded at electrodes (A) modified via covalent attachment of Th-laccase, in O_2 saturated medium.*

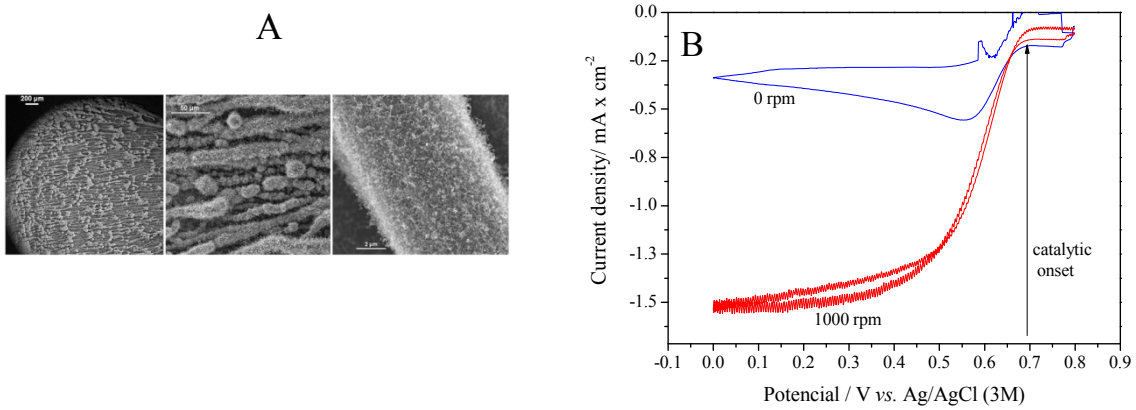

Figure 32. *(A) Adsorption of Lc to the PHA-modified electrode surface. (B) Biocatalytic current recorded at covalently attached AuNPs, modified with ThLc.*

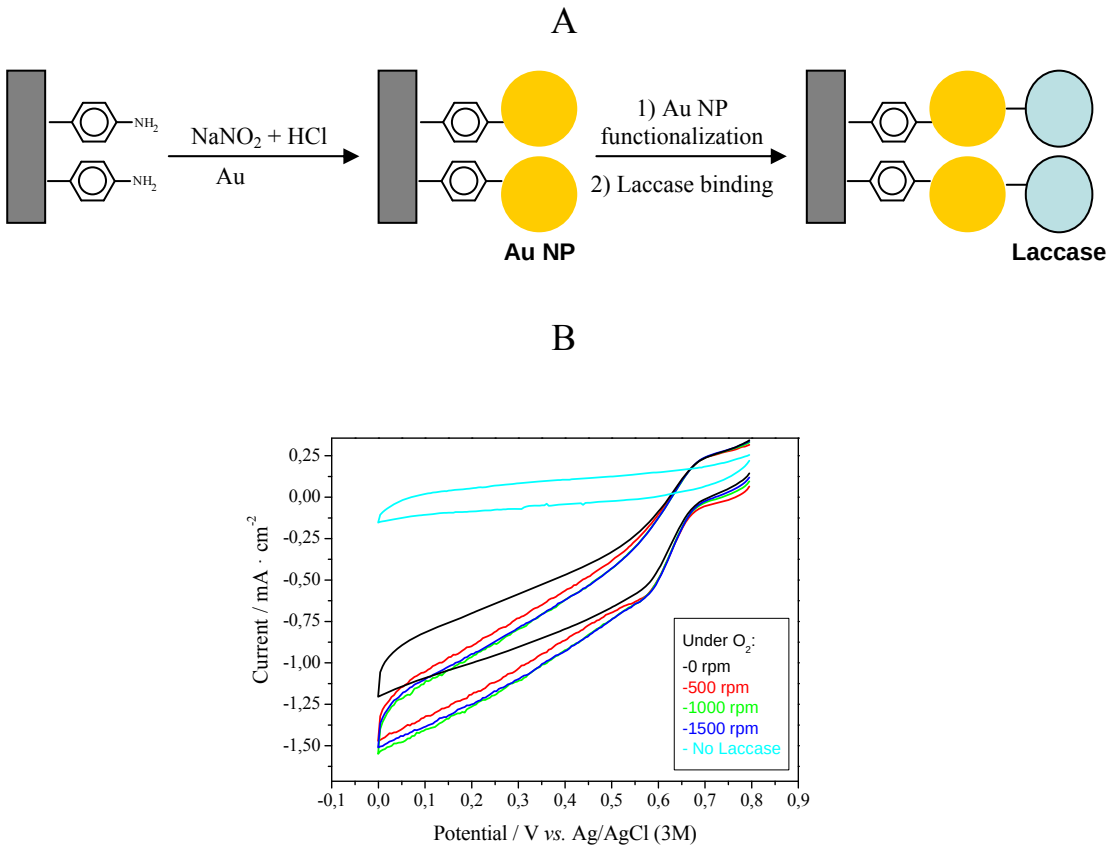

Figure 33. *Rotating disk experiments carried at a similar electrode, showing linear dependends of the current density on square root of angular rotation rates.*

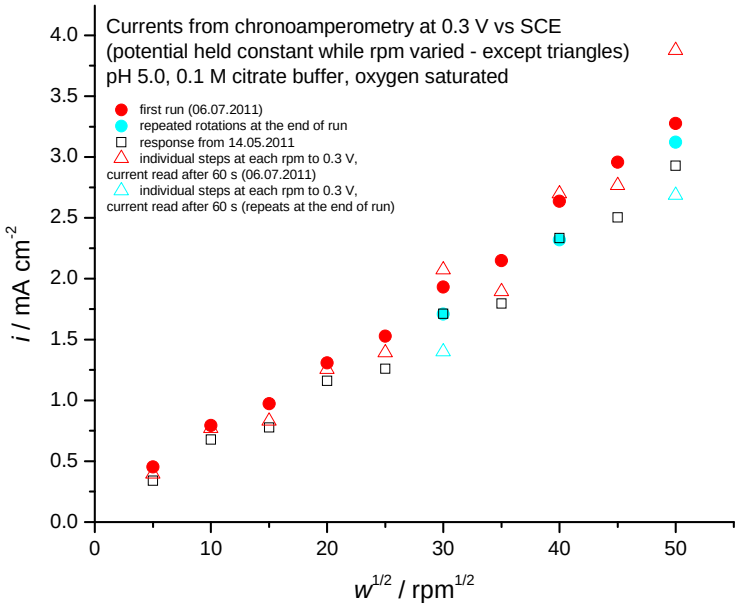

Figure 34. *Calibration graphs (current density) of GcGDH/Os polymer modified graphite electrodes* (5 µ L of GcGDH enzyme, 2 µL of Os polymer, and 1 µL of PEGDGE).

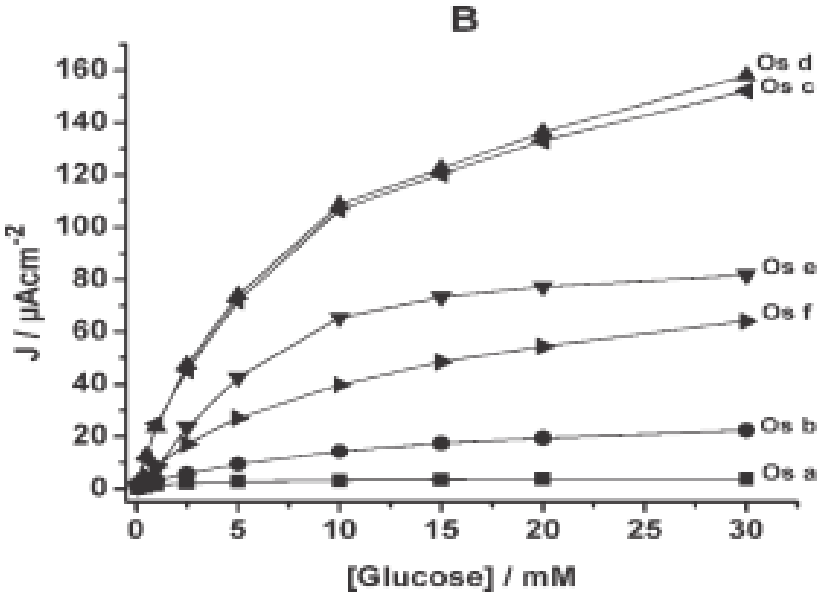

Figure 35. *Schematic representation of a biofuel cell setup with two distinct compartment* (the photo of the setup is inserted).

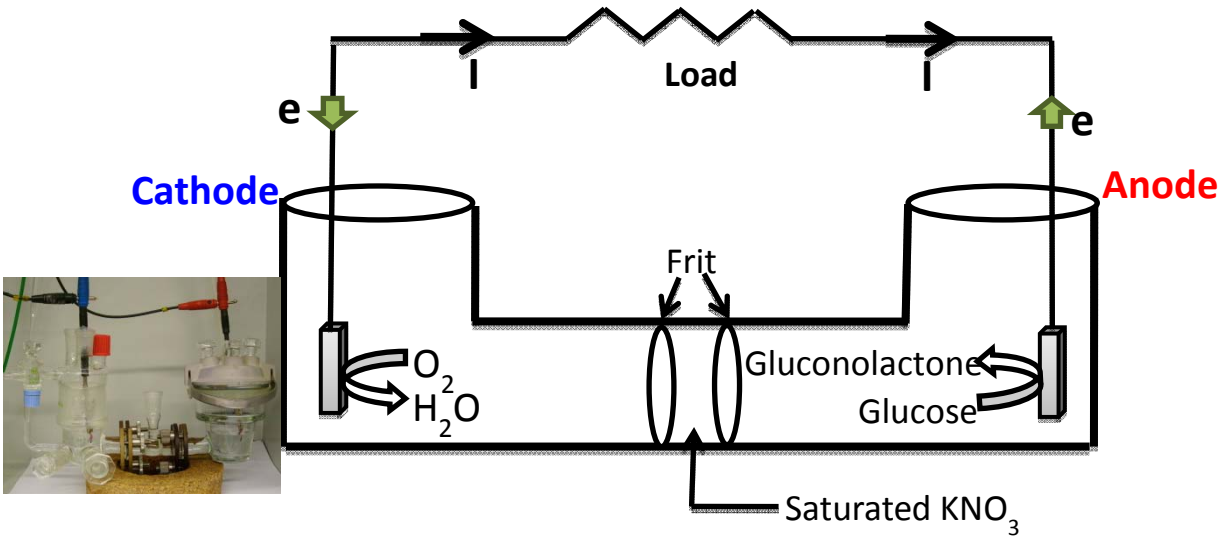

Figure 36. *Typical dependences of power density on operating voltage of BFCs operating in air-saturated quiescent solutions.*
(a) 50 mM phosphate buffer, pH 7.4 containing 100 mM glucose (solid line) and (b) 50 mM phosphate buffer, pH 7.4 containing 5 mM lactose (dashed line).

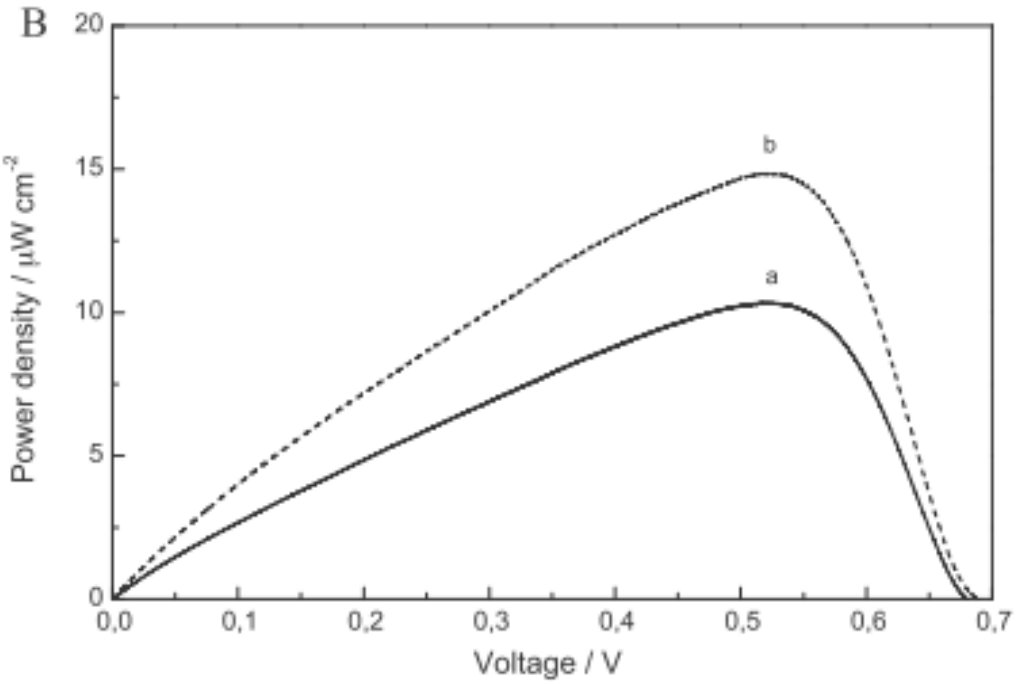

***Figure 37**. Calibration plots for glucose using the developed biosensor based on CtCDH* (linear reange and extended Michaelis-Menten profiles).

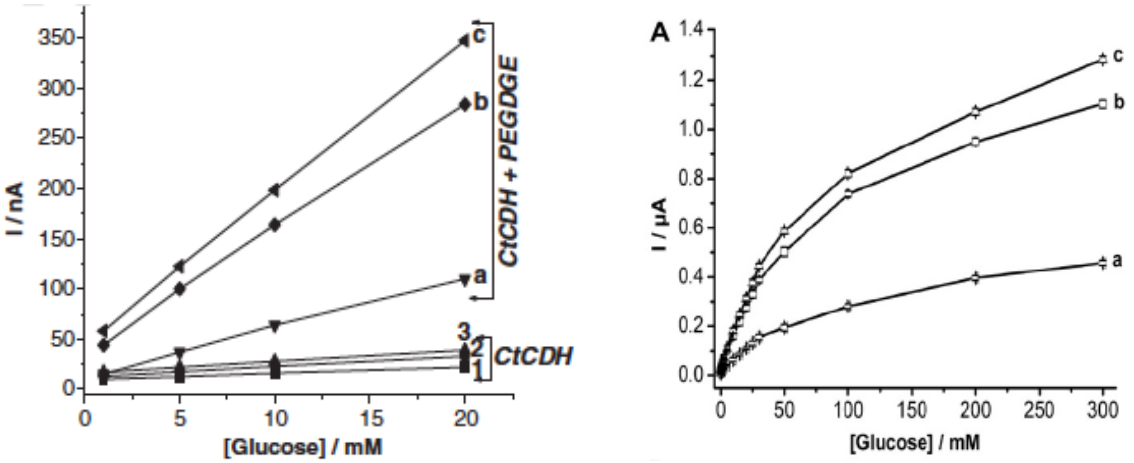

***Figure 38**. Chronoamperometric response of the biosensor towards successive additions of aliquots of buffer solution saturated in pure O_2.*

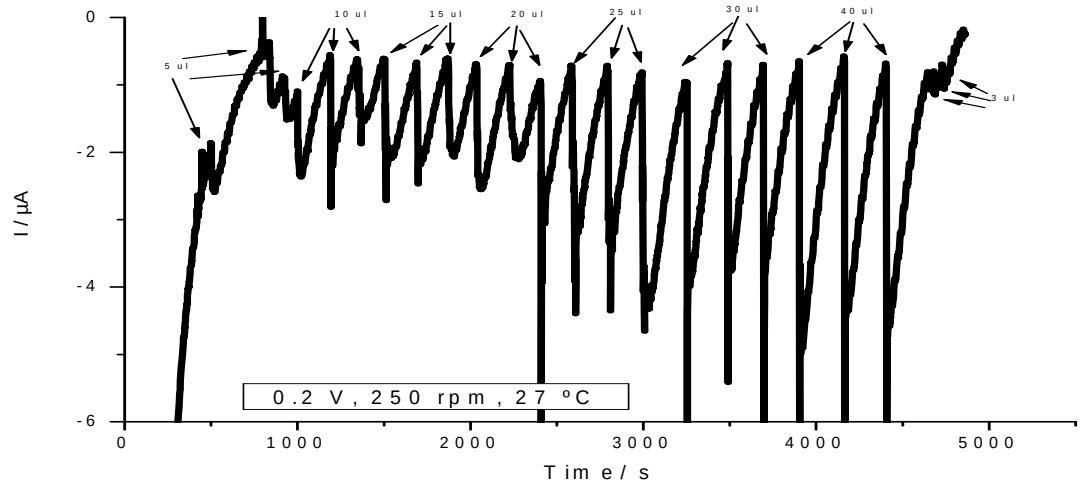

Figure 39. *Concentration dependence of the electrochemical response of the electrode towards O_2.*

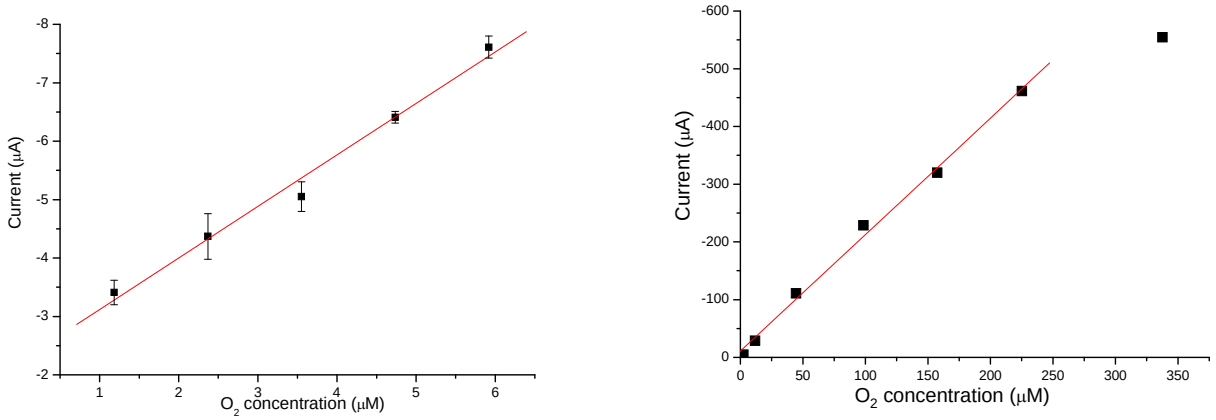

Figure 40. *A short summary of possible bioanodes (up arrows) and biocathodes (down arrows) placed on x-axe of onset potentials and schematically representing demonstrated current densities (length of the arrow) for their combination into a functional biofuel cell fulfilling the device operational conditions of 600 mV cell potential (width of red box) and a generated current of 400 µA.*

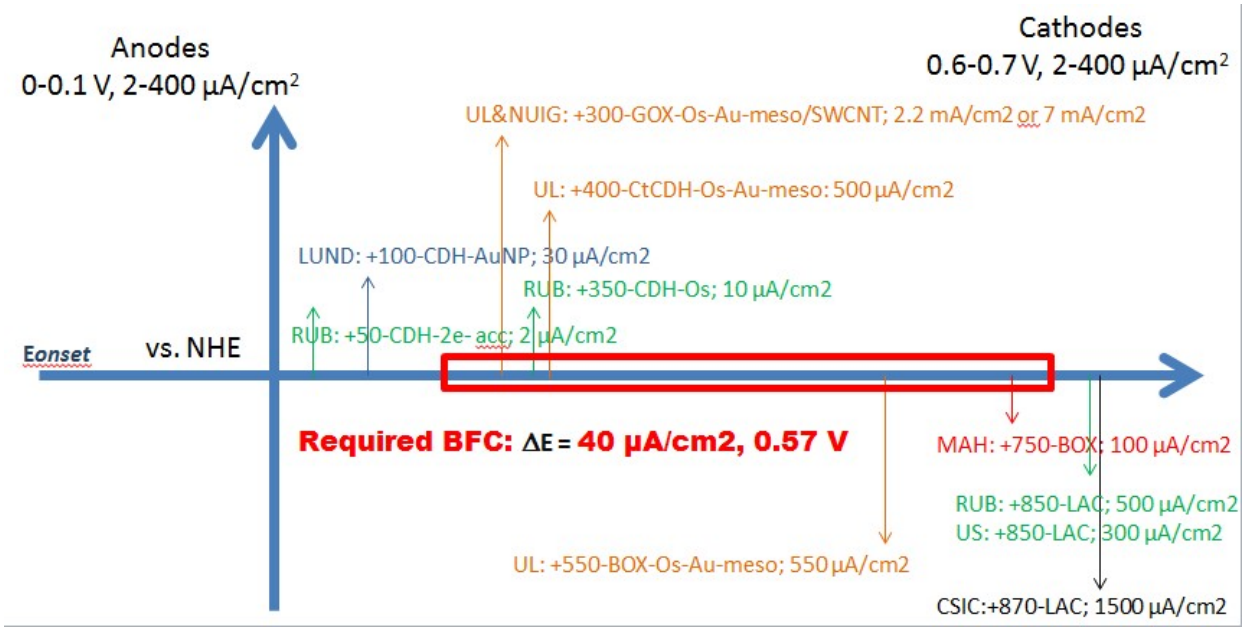

Figure 41. *Block diagram of sensor electronics, blue boxes is energy harvesting module.*

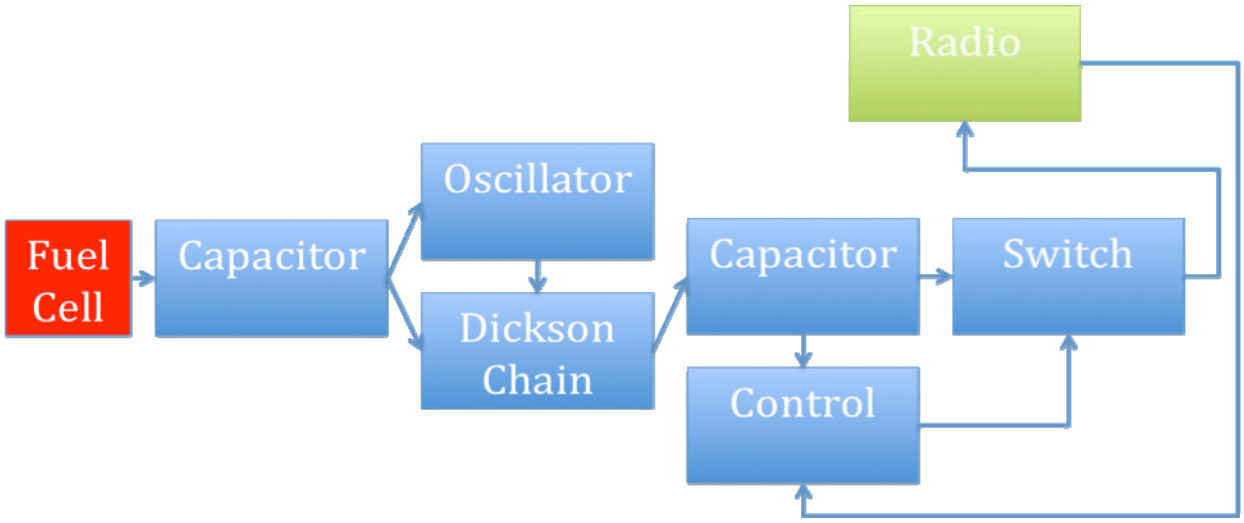

Figure 42. *Sensor signal amplifier*

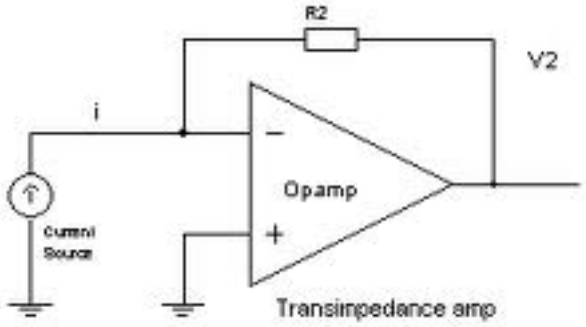

Figure 43. *Timing cycle of sensor, sample, transmit data and sleep all within 4.6 ms.*

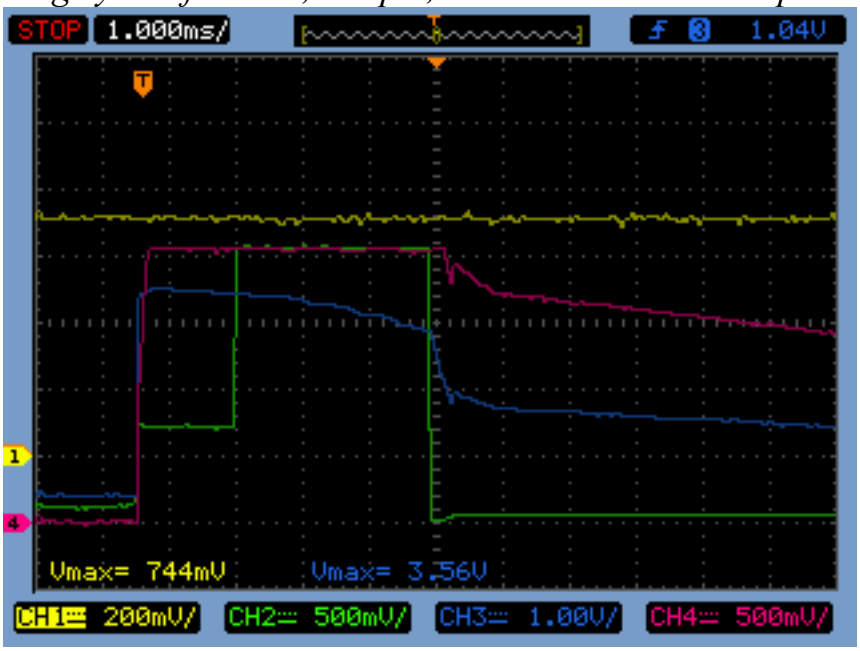

Figure 44. *The sensor sends data to a receiver, which is connected to a computer that extract, store, and display the information.*

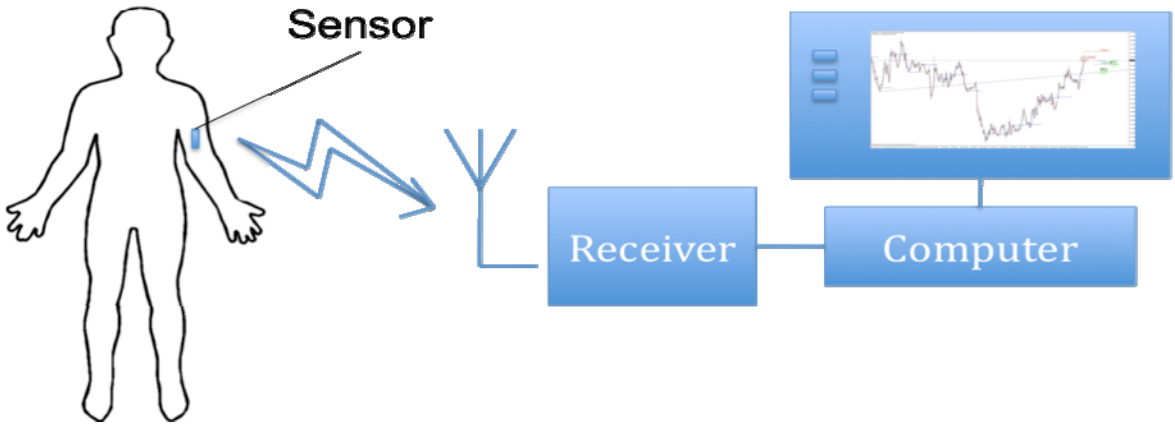

Figure 45. *The sensor setup using a single cell battery for testing the oxygen sensitive device.*

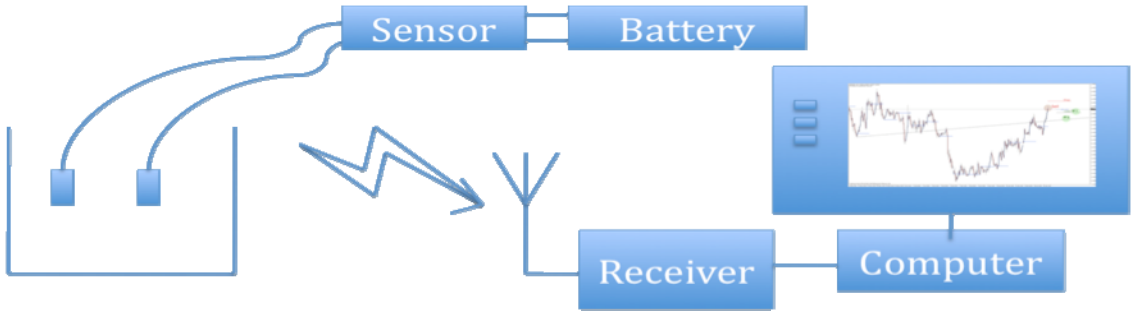

Figure 46. *The setup of electronics for testing the glucose sensitive device*

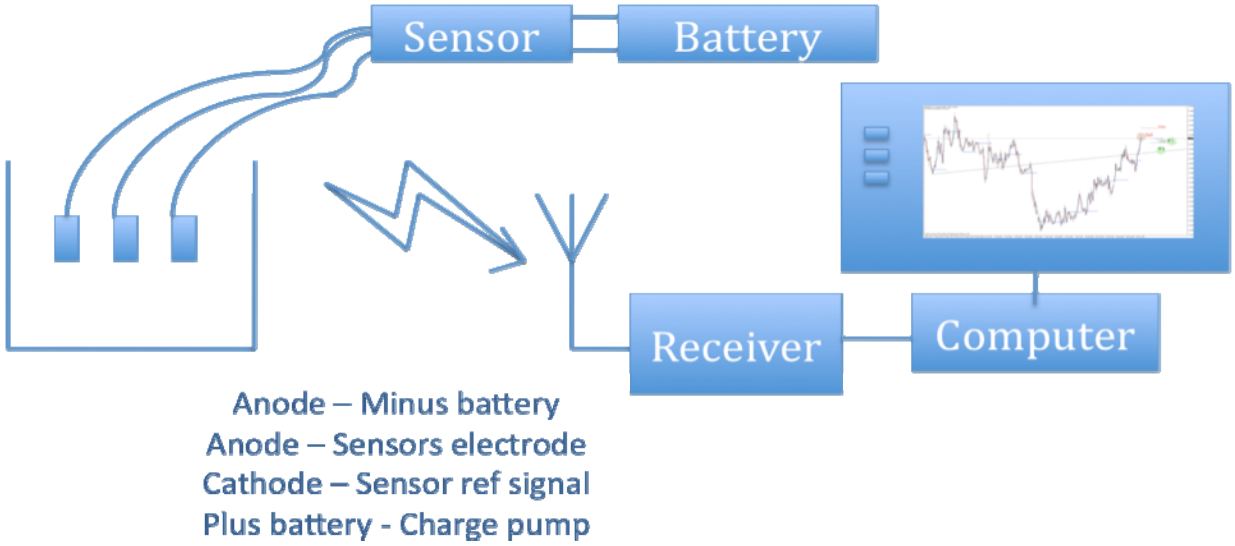

Figure 47. *Data from preliminary tests of wireless self-powered devices (powered by a low voltage battery) for glucose and oxygen monitoring.*
Dashed line represents the background signal from electronics.

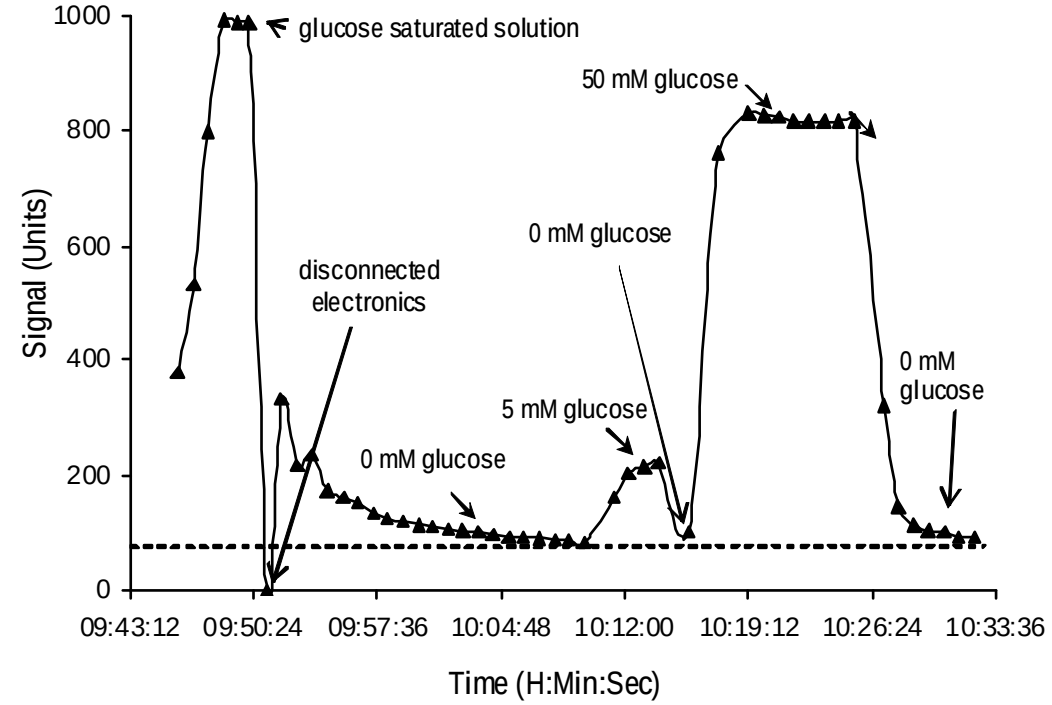

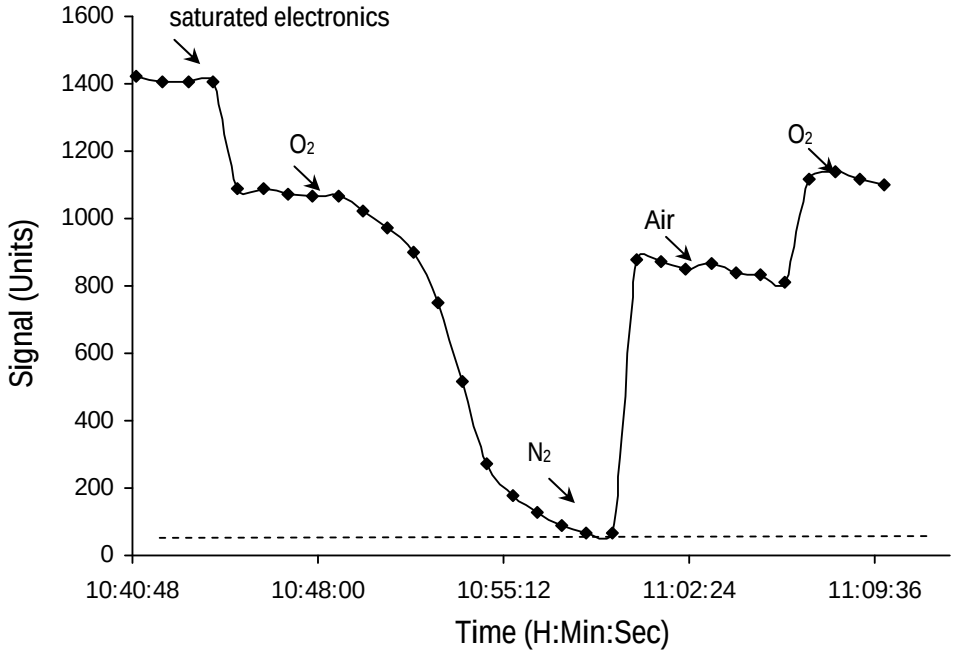

Figure 48. *Data from two final tests of wireless self-powered biodevices for glucose and oxygen monitoring.*